24

Discovery of Biorhythmic Stories behind Daily Vital Signs and Its Application

Wenxi Chen
Biomedical Information Technology Laboratory, the University of Aizu
Japan

1. Introduction

The historical development of the study of biorhythms and the physiological background, as well as functionality of biorhythmic phenomena in human beings, is introduced. The latest achievements in modern chronomedicine, as well as their applications in daily health care and medical practice, are reviewed. Our challenges in monitoring vital signs during sleep in a daily life environment, and discovery of various inherent biorhythmic stories using data mining mathematics are described. Several representative results are presented. Finally, potential applications and future perspectives of biorhythm studies are extensively discussed.

1.1 Historical review

Biorhythmic phenomena are innate, cyclical biological processes or functions existing in all forms of life on earth, including human beings, which respond dynamically to various endogenous and exogenous conditions that surround us (Wikipedia, 2009b). The worldwide history of biorhythmic studies and their application in medical practice can be traced back more than 2000 years, to around a few centuries B.C. Since written records exist in China from more than 4000 years ago, numerous unearthed cultural relics and archaeological materials show that the philosophy of yin and yang and the concept of rhythmic alternation had dominated almost every aspect of Chinese society and people's behaviour (Sacred Lotus Arts, 2009).

Following the philosophy of yin and yang, the earliest existing medical book, "The Medical Classic of Emperor Huang", was formulated from a dialogue between Emperor Huang and a medical professional, Uncle Qi, based on the theory of yin and yang, and compiled from a series of medical achievements by many medical practitioners between 770–221 B.C. The first publication of the book was confirmed to have occurred no later than 26 B.C. and no earlier than 99 B.C. (Wang, 2005).

The book was a medical treatise consisting of a collection of 162 papers in two parts: "Miraculous Meridian and Acupuncture" and "Medical Issues and Fundamental Principles". Each part has nine volumes, and each volume has nine papers, because the number nine is the highest number in Chinese culture, and here, implies that the book covers all aspects of medical matters (Zhang et al., 1995).

This book provided a systematic medical theory and insights into the prevention, diagnosis, and treatment methodologies for diseases. At the same time, the interrelationship between meteorological factors, geographical conditions, and the health of human beings was established and rationalized as the theory of "The unity of heaven and humanity", which considered human beings an integral part of the universe.

This book laid the foundation for Traditional Chinese Medicine (TCM) in terms of fundamental concepts and a theoretical framework, including primary theories, principles, treatment techniques, and methodology. The advent of the book showed that TCM had matured enough to be an independent discipline, such as mathematics, astronomy, or geography, along with the many other scientific achievements in China.

Emperor Huang was considered to be the founder of Chinese civilization, and was the respected supreme authoritative as a Son from Heaven. Later work on the validation and further development of TCM remained to be carried out by many talented TCM successors.

One of the most eminent achievements was contributed by Zhang Zhongjing (ca. 150–219 A.D.) (Wikipedia, 2009g), who is known as the Chinese Aesculapius, and whose works "Treatise on Cold Pathogenic Diseases" and "Essential Prescriptions of the Golden Coffer" established medication principles and provided a summary of his medicinal experience based on his clinical practice and his interpretation of "The Medical Classic of Emperor Huang".

There are three important historical periods in the development and maturation of TCM following Zhang's pioneer work. The first period is from the 3rd to the 10th century, where the main works focused on inheritance, collation, and interpretation of the existing theories described in "The Medical Classic of Emperor Huang". Several milestones in the TCM system were reached in the second period, from the 10th to the 14th century, which is the most important period in the development of TCM. Many medical practitioners studied and annotated the ancient classic, and accumulated their own clinical experiences and proposed their own doctrines. The most eminent representatives were known as "the four great masters": Liu Wansu (1120–1200), Zhang Congzheng (1156–1228), Li Gao (1180–1251), and Zhu Zhenheng (1281–1358). Their contributions greatly enriched and accelerated the development of TCM. Further development and many practical medication approaches were matured in the third period, from the 14th to the 20th century.

Wu Youke (1582–1652) published "On Plague Diseases" in 1642, summarizing his successful fight against pestilence during periods of war, and proposed a theory on the cause of disease and pertinent treatments, which was a significant breakthrough in aetiology akin to modern microbiology.

Based on the "Herbal Classic of Shennong", which described medication using mainly herbal plants, as many as 365 components (252 plants, 67 animals, and 46 minerals), Li Shizhen (1518–1593) spent 29 years writing the "Compendium of Materia Medica", which identified herbal medication into 1892 classifications in 60 categories, and formulated more than 10,000 prescriptions.

The "Detailed Analysis of Epidemic Warm Diseases", written by Wu Jutong (1758–1836), was published in 1798. Many prescriptions described in this book are still considered to be effective, and are used in present clinical practice.

The more than 2000 years of TCM history were created and shaped by numerous medical practitioners through constant exploration and sustained innovation, starting with "The Medical Classic of Emperor Huang", which was built from a very simple philosophy, yin

and yang theory, just like modern computer science is built on a "one and zero" platform (Wikipedia, 2009f).

As shown in Figure 1, yin and yang represents two sides of everything, and governs all aspects of cosmic activities and phenomena in the universe. Constant alternation of the yin and yang status is the origin of universal dynamics. The two sides can coexist, be complementary, mutually inhibitable, mutual transformable, and inter-inclusive.

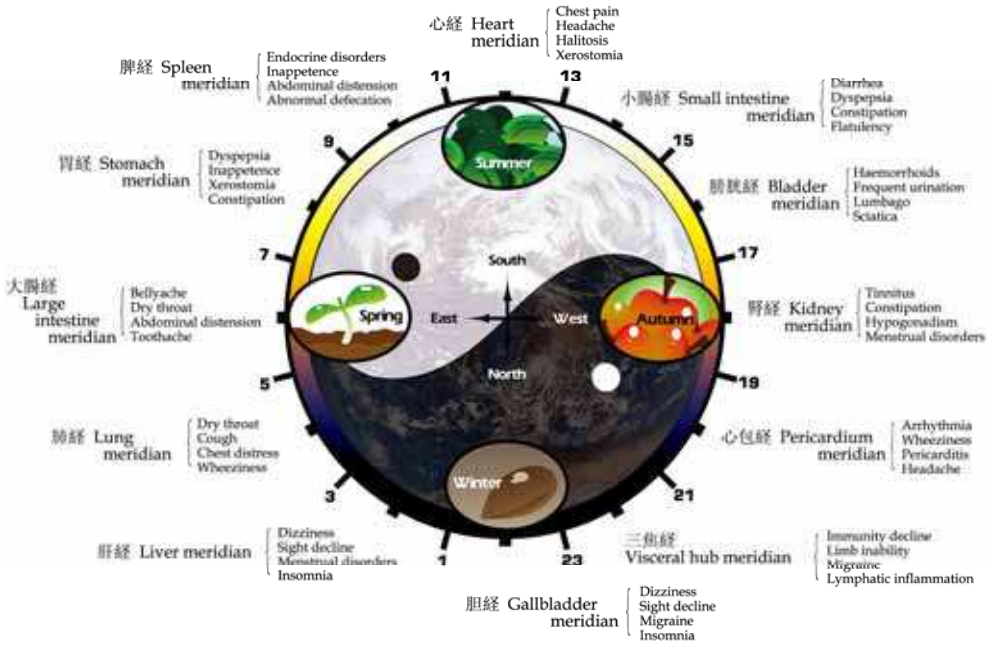

Fig. 1. A holistic overview of the TCM system. On-duty organic meridians in human beings, and disease vulnerabilities in different time domains, and their interaction with various exogenous aspects, such as meteorological, environmental, geographical, and temporal factors from daily to seasonal and yearly, are illustrated (visualization based on Wang, 2005 and Zhang et al., 1995).

TCM considers that a subtle energy ("Qi" in TCM) and blood kinetics in the human body can be expressed as yin and yang alternation corresponding to the waxing and waning periodicities of the sun and the moon. Human moods, health, and behaviour are modulated by the ebb and flow of yin and yang. Human behaviour must synchronize with the natural time sequence to maintain the "Qi" in a good dynamic balanced condition between the yin and yang status.

TCM insists that an unbalance between the yin and yang status is the essential cause of the incidence and exacerbation of disease. The goal of treatment is, in principle, to restore and maintain the balance between yin and yang among the visceral organs. A holistic balance between yin and yang indicates the health status. The yin and yang status can be affected by various endogenous and exogenous factors. The former includes emotional, psychological,

and behavioural aspects, and the latter includes meteorological, environmental, geographical, and temporal factors. Once the yin and yang falls into unbalance, i.e., excess or deficiency on either side, this induces disease. TCM persists from an integrative and holistic standpoint in terms of methodology and philosophy to explain health and disease issues as a result of interaction with many endogenous and exogenous aspects that surround us.

The theories of "syncretism of body and mind" and "the harmony of human with nature" in TCM consider that not only are mental and physical health interconnected, but also vital body functions are modulated by the environmental and seasonal variations due to the movement of the earth and sun and the waxing and waning of the moon over a year. For example, mental disorders, such as excess mood swings in joy, anger, worry, fright, shock, grief, and pensiveness, may affect the visceral organs directly. Depression disrupts the normal functions of the spleen and stomach. Marked changes in weather conditions, such as dryness, dampness, cold, heat, wind, and rain, can induce an unbalance in yin and yang and lead to disease.

TCM considers that an inseparable relationship exists between humans and nature, from birth, development, maturation, caducity, and death, just as seasonal alternations, waxing, and waning occur in the universe. Life activities must be synchronized with natural rhythms to reach harmonic status and maintain longevity. To obtain sufficient sunlight, to ward off chilly north winds, and to enjoy all amenities, the recommended habitation is for a house to sit the north and face the south, back onto mountains, and be close to water.

One of the most prominent features in TCM is the temporal concept in treating health and disease. Spring, summer, autumn, and winter imply burgeoning, growth, harvest, and reposition in nature, respectively. Following a seasonal alternation in work and life is the key to maintaining good health for human beings. Sleep is emphasized as being important as exercise, breathing, and meals in maintaining a normal life activity. A single night's sleeplessness may require 100 days to recover. The daily sleeping–waking cycle should follow the regular celestial mechanics. People should go to sleep late and get up early during the spring season, when all is recovering from the winter hibernation. Acupuncture treatments stipulate strict needle selection in terms of their geometric shape, position, and depth for different seasons using a series of precise instructions.

Because not only physiological and pathological functions, but also the severity of a disease and the effectiveness of its diagnosis/treatment are time-dependent from a TCM standpoint, a day is divided into four parts. From midnight to 6:00 a.m., yin begins to fade from its peak, and yang gradually increases. From 6:00 a.m. to noon, yin finally fades away and yang gradually reaches its peak. From noon to 6:00 p.m., yang begins to fade from its peak and yin gradually increases. From 6:00 p.m. to midnight, yang finally fades away and yin gradually reaches its peak. Most diseases become more severe after dusk when yin increases, and mitigate in daytime when yang dominates.

A day is further divided into 12 time slots. Individual organ-related meridians alternate in being on-duty in each time slot. As shown in Figure 1, many ailments and diseases have their own time-dependent features, which should be taken into consideration in diagnosis and treatment. Different diseases are related to different meridians, and the treatment should be targeted to the on-duty meridian. Patients with liver disease are usually better in the morning, exacerbate between 3:00–5:00 p.m., and become calmer at midnight. Patients with heart disease are calm in the morning, feel comfortable at noon, and become

exacerbated at midnight. Patients with spleen disease show severe symptoms at sunrise, are calm between 3:00–5:00 p.m., and feel better at sunset. Patients with lung disease show severe symptoms at noon, feel better between 3:00–5:00 p.m., and are calm at midnight. Patients with kidney disease feel better at midnight and are calm in the early evening, but become aggravated during four time slots (1:00–3:00 a.m., 7:00–9:00 a.m., 1:00–3:00 p.m., and 7:00–9:00 p.m.)(Wikipedia, 2009d; Ni, 1995; Veith, 2002).

Identifying the root cause of the disease is a very important part of TCM practice. TCM stresses that balance is the key to a healthy body. Any long-term imbalance, such as extreme climate change, undue physical exercise, heavy workload, excessive rest, too frequent or rare sexual activity, unbalanced diet, or sudden emotional changes can all cause disease (Xuan, 2006).

A holistic view of the human body is not the sole understanding of the TCM system. In approximately the same historical period on the other side of the earth, Hippocrates (ca. 460–ca. 370 B.C.), a Greek physician known as "the father of medicine", laid the foundations of Western medicine by freeing medical studies from the constraints of philosophical speculation and religious superstition.

"The Hippocratic Corpus" is a collection of about 60 treatises believed to have been written between 430 B.C. and 200 A.D. by different people under the name of Hippocrates (Naumova, 2006). The corpus describes many points of view on diseases related to temporal and environmental factors, such as:

- As a general rule, the constitutions and the habits of people follow the nature of the land where they live.
- Changes in the seasons are especially liable to beget diseases, as are great changes from heat to cold or cold to heat in any season. Other changes in the weather have similar severe effects.
- When the weather is seasonable and the crops ripen at regular times, diseases are regular in their appearance.
- Each disease occurs in any season of the year, but some of them occur more frequently and are of greater severity at certain times.
- Some diseases are produced by the manner of life that is followed, and others by the life-giving air we breathe.

As a pioneer in studying biorhythms, an Italian physician, Santorio Santorio (1561–1636), invented a large "weighing chair" to observe the weight fluctuations in his own body during various metabolic processes, such as digestion, sleep, and daily eating over a 30-year period (Wikipedia, 2009e). He reported the circadian variation both in body weight and in the amount of insensible perspiration in his book "On Statistical Medicine", published in 1614, which introduced a quantitative aspect into medical research, and founded the modern study of metabolism.

In 1729, a French astronomer named Jean Jacques Ortous de Mairan (1678–1771) devised a classical circadian experiment. He placed a heliotropic plant in the dark and observed that the daily rhythmic opening and closing of the heliotrope's leaves persisted in the absence of sunlight (Wikipedia, 2009c). We now understand that the circadian clock controls given processes, including leaf and petal movements, the opening and closing of stomatal pores, the discharge of floral fragrances, and many metabolic activities in plants.

Christopher William Hufeland (1762–1836), a German physician, published "The Art of Prolonging Life" in 1796. He stated that "The life of man, physically considered, is a peculiar

chemico-animal operation; a phenomenon effected by a concurrence of the united powers of Nature with matter in a continual state of change." He considered that the rhythmicity of twenty-four hours is formed by the regular revolution of our earth, and can be seen in all diseases, and all the other biorhythms are determined by it in reality (Hufeland, 1796).

In the early 19th century, identical conclusions from investigations into biorhythms from different approaches and from independent researchers in different fields, such as psychology and meteorology, were reached.

In his book "Die Perioden des Menschlichen Organismus (Periodicity in the Life of the Human Organism)", the Austrian psychologist Hermanna Swoboda stated that, "Life is subject to consistent changes. This understanding does not refer to changes in our destiny or to changes that take place in the course of life. Even if someone lived a life entirely free of outside forces, of anything that could alter his mental and physical state, still his life would not be identical from day to day. The best of physical health does not prevent us from feeling ill sometimes, or less happy than usual". By analysing dreams, ideas, and creative impulses of his patients, Swoboda noticed very regular rhythms with predictable variations in some artists' performances and the mental status of pregnant women (Biochart Com, 2009).

Even the influence of meteorological factors, such as sunspot activity, was associated with the acute chronic diseases of the heart, blood vessels, liver, kidney, and nervous system, ranging from mild to severe, such as excitability, insomnia, tiredness, aches, muscle twitches, polyuria, digestive troubles, jitteriness, shivering, spasms, neuralgia, neural crises, asthma, dyspnea, fever, pain, vertigo, syncope, high blood pressure, tachycardia, arrhythmia, and true angina pectoris (Vallot et al., 1922).

In 1924 and 1928, Alexander Chizhevsky (1897–1964) published "Epidemiological Catastrophes and the Periodic Activity of the Sun" and "Influence of the Cosmos on Human Psychoses", respectively, studying biorhythms in living organisms in their connections with solar and lunar cycles, stating that, "Life is a phenomenon. Its production is due to the influence of the dynamics of the cosmos on a passive subject. It lives due to dynamics, each oscillation of organic pulsation is coordinated with the cosmic heart in a grandiose whole of nebulas, stars, the sun and the planet", which is now formulated as the independent discipline of "heliobiology" (Wikipedia, 2009a).

1.2 Modern chrono-related studies

In the 1950s, Franz Halberg noticed that the eosinophil counts of both sighted and blinded groups of mice rose and fell cyclically with temperature variations. In the former group, this occurred at approximately the same time each day, and in the latter group, there was a slight shift and a shorter cycle. Neither group showed an exact 24-hour cycle, showing the existence of an endogenous mechanism (Halberg et al., 1959).

When the implications of these cycles were explored further, it was found that one group of mice developed seizures when exposed to an extremely loud noise at 10:00 p.m., the active period of their day, while another group that was exposed to the noise at noon, during their rest period, did not develop seizures. It was also found that when a potential poison or high doses of a drug were given to mice, whether they lived or died depended on the delivery time of the drug.

The study of the body's time structure was continued in the late 1960s by Halberg and his Indian co-researchers in medical practice by administering radiation therapy to patients

with large oral tumours. The tumour temperature was used as a marker to schedule treatments. Patients were divided into five groups and treated at a different time offset, –8, –4, 0, +4 and +8 hours, from their peak temperature. More than 60% of patients who received treatment when the tumour was at peak temperature were alive and disease-free two years later. This is perhaps because the highest metabolic activity at peak temperature enhanced the therapeutic effect (Halberg, 1969).

An increased swing in the amplitude of blood pressure, which develops before a rise in mean blood pressure, was found in rats (Halberg, 1983). In 1987, this phenomenon was confirmed to be a greater risk factor for ischemic stroke from a six-year study involving nearly 300 patients (Halberg & Cornélissen, 1993). This is now known as circadian hyper amplitude tension (CHAT). CHAT studies have shown that taking blood pressure medication at an undesirable time can cause CHAT, and can potentially lead to a stroke.

In addition to body temperature and blood pressure, biorhythmic variations in other vital signs, such as saliva, urine, blood, and heart rate, have been quantified to identify normal and risky patterns for disease, to optimize the timing of treatment, and to compare variations among subjects grouped by age and gender (Halberg et al., 2003; Halberg et al., 2006a; Halberg et al., 2006b).

In 1960, the nascent field of biorhythm studies celebrated its first symposium in New York, USA, and modern chrono-related studies are now expanding in both dimensional and functional scales, from the genome level to the whole-body level, and from fundamental chronobiology to medical applications, such as chronophysiology, chronopathology, chronopharmacology, chronotherapy, chronotoxicology, and chronomedicine. All of these topics are rooted in the study of biorhythmic events in living organisms and their adaptation to solar- and lunar-related rhythms, and are still in the exciting process of discovery.

Although rhythmic phenomena in many behavioural and life processes, such as eating, sleeping–waking, seasonal migration, heart-beat, and cell proliferation, had been observed in many aspects for a long time, little was known about their physiological background until recent advances in molecular biology and genetics. Scientists have now identified specific genes, proteins, and biochemical mechanisms that are responsible for spontaneous oscillations with rhythmic cycles extended from the molecular, cellular, tissue, and system levels on a spatial scale, from the millisecond intervals of neuronal activity to seasonal changes in the temporal scale (Martha & Sejnowski, 2005).

The suprachiasmatic nucleus (SCN), composed of 20,000 or so autonomous cells located in the hypothalamus, is now known to be responsible for controlling the timing of endogenous rhythms (Stetson & Watson-Whitmyre, 1976). The SCN receives an environmental input, such as light, a type of zeitgeber, from light receptors in the retina via the retinohypothalamic tract (RHT), and generates a rhythmic output to coordinate and synchronize body rhythms. The SCN is fundamental to each of the three major clock components in biological systems: entrainment pathways, pacemakers, and output pathways to effecter systems (Reppert & Weaver, 2001). Autonomous single-cell oscillators reside in peripheral tissues as well as in the SCN of the pineal gland. Peripheral oscillators may respond more directly to environmental factors, such as temperature, moisture, pressure, and sound. However, the SCN governs and coordinates the rhythms of the peripheral oscillators by both direct neural connections and diffusible biochemical processes (Balsalobre et al., 2000). As a result of such synchronization, the body as an entire system

maintains rhythms for not only the sleeping–waking cycle, but also for body temperature, heart rate, blood pressure, immune cell count, and hormone secretion levels, such as cortisol for stress and prolactin for immunity and reproduction. Rhythmic beating in the SCN is the timepiece not only for daily cycles, but also for the totality of lifelong personal patterns, potentially in a harmonic resonance with the environmental surroundings.

The clock genes are expressed not only in the SCN, but also in other brain regions and various peripheral tissues. The liver has been confirmed to be a biological clock capable of generating its own circadian rhythms (Turek & Allanda, 2002). A microarray analysis experiment has revealed that there are many genes expressing a circadian rhythm in the liver. The relative levels of gene expression in the liver of rats have been investigated from the viewpoint of the time of day. Sixty-seven genes were identified where their expression was significantly altered as a function of the time of day, and these were classified into several key cellular pathways, including drug metabolism, ion transport, signal transduction, DNA binding and regulation of transcription, and immune response according to their functions (Desai et al., 2004).

In the cases where exogenous cues (zeitgebers) for timing, such as light, temperature, or sound, are shielded, the SCN moves out of synchronization with the exogenous entrainment. However, the innate rhythm is not obliterated, because biorhythms are genetically built into cells, tissues, organs, and the whole-body system. The body still maintains its rhythms, but not in an organized tempo. The sleeping–waking cycle and body temperature variation will not follow an exact 24-hour cycle, which was entrained by the light–dark cycle or the sunset–sunrise cycle. Other biorhythms and daily activities could also be affected, although none has all its variables equal.

The broad spectrum of different biorhythms is classified into three categories, i.e., circadian rhythms, ultradian rhythms, and infradian rhythms.

The circadian rhythm is the most common biorhythm, alternates in an approximately daily cycle, and exists in most living organisms. The term "circadian" comes from circa, which means "about", and dies, which means "day".

Ultradian rhythms refer to those cyclic intervals that are shorter than the period of a circadian rhythm, exhibiting periodic physiological activity occurring more than once within a day, such as neuron firing, heart-beats, inhalation and expiration, and REM–NREM sleep cycles.

Infradian rhythms pertain to regular recurrences in cycles of longer than the period of a circadian rhythm, and occur on an extended scale from days to years. Some of these are listed below:

- Circasemiseptan rhythms have a cyclic length of 70 to 98 hours or 3.5 days, and exist in blood pressure and heart rate fluctuations. They can be found in patients with incidence of myocardial infarction and apoplexy.
- Circaseptan rhythms occur in periods of 140 to 196 hours or about one week, and are found in changes in body temperature and blood pressure.
- Circatrigintan rhythms behave in approximately monthly cycles. The most common is the female menstrual cycle, ranging from 25 to 35 days. Others include the emotional and physical stamina rhythms, which change over 28 days and 23 days, respectively. Intellectual rhythmicity was found to exhibit a regular 33-day cycle for mental agility and ability. The existence of a 21-day cycle related specifically to moods was uncovered.

Some vital signs, such as hormone secretion, blood pressure, and metabolic activity, have similar properties.

- Circannual rhythms occur over a period of between 305 to 425 days, or about a year. Most plants have a seasonal change from rootage, burgeon, blossom, and fructification. Migratory birds migrate in an annual pattern through regular seasonal journeys in response to changes in food availability, habitat, or weather.

Table 1 summarizes various known biorhythms ranging from periods of milliseconds to years that exist in living organisms.

Biorhythm		Cycle length	Related event
Ultradian		< 1 d	Neuron firing, heart beating, inhalation and expiration, REM–NREM sleep cycles
Circadian		1 d ± 4 h	Body temperature (BT), blood pressure (BP), heart rate (HR), hormone secretion
Infradian	Circadidian	2 ± 0.5 d	Body weight, urine volume
	Circasemiseptan	3.5 ± 1 d	Sudden death
	Circaseptan	7 ± 1.5 d	Rejection of heart transplant, activity, BP, BT
	Circadiseptan	14 ± 3 d	Body weight, grip strength
	Circavigintan	21 ± 3 d	Mood, 17-ketosteroid excretion
	Circatrigintan	28 ± 5 d	Emotional and physical stamina, mental agility and ability, menstruation
	Circannual	1 y ± 2 m	BP, aldosterone
	Circaseptennian	7 ± 1 y	Marine invertebrates
	Circaduodecennian	12 ± 2 y	BP
	Circadidecadal	20 y	BP

Table 1. Temporal definitions and the properties of diversified biorhythms ranging from periods of milliseconds to years (adapted from Halberg & Cornélissen, 1993; Koukkari & Sothern, 2006). Cycle length: h = hours; d = days; m = months; y = years.

Objective estimation of various biorhythmicities in different physiological vital signs and biochemical biomarkers, such as body temperature, heart rate, blood pressure, adrenocorticotropic hormone, and melatonin, is indispensable in medical practice. Many vital signs and biomarkers are usually modulated and interacted by multiple biorhythms. Similarly, multiple biorhythms are often interwoven within a vital sign or a biomarker as shown in Table 1. Because biorhythms are cyclic, recurring physiological events, their features in time structures are commonly expressed by parameters such as period, mesor,

amplitude and phase, zenith and nadir, onset of events, the minimum and maximum incidence of events, and the shape of the rhythmic pattern.

Mathematical approaches to quantifying biorhythms were classified into two categories in the early stages of their study: macroscopic and microscopic (Halberg, 1969). The former category employs many statistical techniques, such as histograms, mean, median, mode, and variance. The latter category uses chronograms, variance spectrum, auto/cross correlations, coherency, and the cosinor method.

The cosinor method uses least-squares criteria to fit raw data on a presumptive single sine wave model in the time domain. Its variants, such as population mean-cosinor, group mean-cosinor, multi-cosinor and non-linear cosinor methods, are similarly based on various compound models (Nelson et al., 1979). The multivariate method has also been used for the parameter estimation of biorhythms in human leukocyte counts in microfilariasis infection (Kumar et al., 1992).

In addition to living organisms, the biosphere and the solar system are good examples of self-tuning control systems. The laws governing the operation of control systems are incorporated in the development of mathematical methods for the identification of rhythms hidden in the dynamics of biological and heliogeophysical variables (Chirkova, 1995).

Fourier transformation and spectral analysis methods have also been developed to evaluate and analyse biorhythms regarding their general characteristics in terms of amplitude, phase, periodical frequency, and cyclic length (Chou & Besch, 1974).

The determination of biorhythms is helpful not only in clarifying their impact on the pathophysiology of diseases, but also in elucidating the pharmacokinetics and pharmacodynamics of medications.

Figure 2 shows the circadian properties of various physiological vital signs and biochemical markers, in alignment with time-dependent symptoms or events of diseases that are in either the severest timing or the most frequent incidence of the disease.

As shown in Figure 2, allergic rhinitis is typically worse in the early waking hours than later during the day. Asthma usually occurs more than 100 times more in the few hours prior to awakening than during the day. Angina commonly occurs during the first four to six hours after awakening. Hypertension typically occurs from late morning to middle afternoon. Rheumatoid arthritis is most intense upon awakening. Osteoarthritis worsens in the afternoon and evening. Ulcer disease typically occurs after stomach emptying, following daytime meals, and in the very early morning, often disrupting sleep. Epilepsy often occurs only at individual particular times of the day or night (Smolensky & Labrecque, 1997).

The daily variation pattern of the symptoms of diseases and biochemical-pathophysiological processes is now used to optimize treatment of various diseases, such as asthma, cancer, diabetes, fibromyalgia, heartburn, and sleep disorders. Chronopharmacokinetic studies have been reported for many drugs in an attempt to explain chronopharmacological phenomena, and these have demonstrated that the time of administration is a possible factor in the variation in the pharmacokinetics of a drug. Time-dependent changes in pharmacokinetics may proceed from the circadian rhythm of each process, e.g., absorption, distribution, metabolism, and elimination. Thus, circadian rhythms in gastric acid secretion and pH, motility, gastric emptying time, gastrointestinal blood flow, drug protein binding, liver enzyme activity and/or hepatic blood flow, glomerular filtration, renal blood flow, urinary pH, and tubular resorption play a role in such pharmacokinetic variations (Labrecque & Belanger, 1991). More than 100 drugs, such as cardiovascular agents, anti-

asthmatic agents, gastrointestinal agents, non-steroidal anti-inflammatory agents, and anti-cancer agents, have already been recognized as exhibiting circadian variations in pharmacokinetic and pharmacodynamic performance over a period of 24 hours (Lemmer, 1994). Chronotherapeutic principles are realized through innovative drug delivery technology in the safe and efficient administration of medications (Smolensky & Labrecque, 1997).

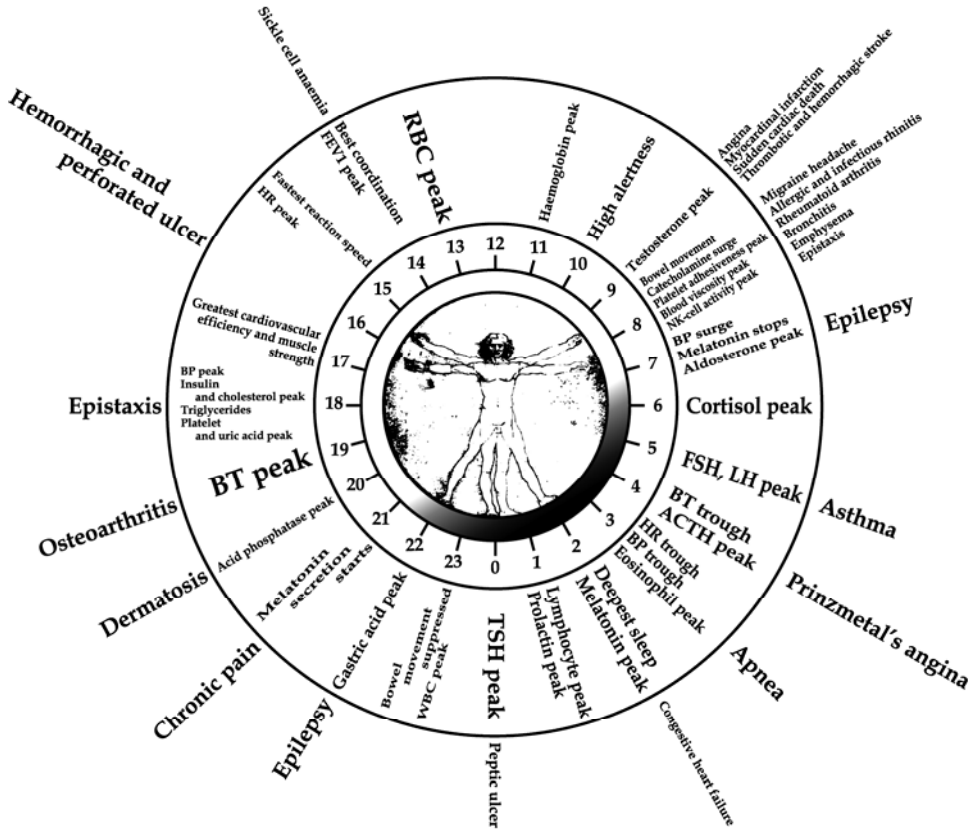

Fig. 2. Circadian rhythmic changes of physiological vital signs and biochemical markers, and symptoms or events of diseases in the case of worst timing or highest likelihood (adapted from Smolensky & Labrecque, 1997; Ohdo, 2007). The outer ring indicates the symptom and disease. The inner ring indicates vital signs and biomarkers.

Other applications utilizing biorhythms can be found in health care, human welfare, and behavioural administration domains. A conventional alarm clock is usually set in advance to sound a bell or buzzer at a desired hour. During the Stage 1 period of sleep, a person drifts in and out of sleep, and can be awakened easily. However, it is very difficult to be woken up during deep sleep periods, such as Stages 3 and 4. When a person is awakened during deep sleep stages, it is difficult for them to adapt immediately, and they often feel groggy and

disoriented for several minutes after waking. A biorhythm-based bell device, biological rhythm-based awakening timing controller (BRAC), was developed to estimate biorhythm changes in sleep cycles from fingertip pulse waves, and was used to optimize the alarm timing (Wakuda et al., 2007).

Jet lag is a malaise often associated with long-distance travel across several time zones. Some of the symptoms usually reported are fatigue, drowsiness, irritability, inability to concentrate during the day, difficulty in sleeping at night, and gastrointestinal discomfort (Katz et al., 2001). Shift workers, such as truck drivers and emergency medical personnel, who are obliged to work non-standard office hours, exhibit similar symptoms to those of jet lag.

Sufferers of jet lag and shift workers are affected by a transient misalignment of the circadian clock with the external clock. Both disorders have a common cause in aetiology, but a major difference exists between the two situations. A long-distance traveller can resynchronize their internal clock within a few days after their biorhythm is disturbed because their internal clock is out of phase with the external clock of sunrise and sunset. By contrast, as long as the daily work schedule of a shift worker cannot be synchronized with the natural biorhythms, they will be unable to truly adapt their biorhythms to the external clock. Although effective treatment has not been rigorously documented yet, the symptoms are usually treated using a light therapy method, for example, artificial light reversal of day and night, which can be attained by subjecting the patient to bright artificial light at night and avoiding photoic stimulation during sunlight hours by wearing sunglasses or closing window curtains (Smolensky & Lamberg, 2000).

It has also been shown that although the exact timing varies from individual to individual, performance in physical and intellectual activities exhibits a daily rhythmicity. The best performance is achieved around the peak body temperature time, which usually occurs in the late afternoon, although overall performance in real world situations can be affected by many other factors, such as innate and acquired skills, motivation, concentration, and spot exertion (Dunlap et al., 2004).

Biorhythmicities are recognized as affecting numerous physiological and behavioural processes. The daily pattern of human activity and stress amplifies the innate biological variability of biorhythms, and diseases can alter the expression and characteristics of circadian and other biorhythms. The outcomes of the chronotherapeutic treatment of several diseases that have predictable circadian variations, such as allergic rhinitis, angina pectoris, arthritis, asthma, diabetes, epilepsy, hypertension, dyslipidemia, cancer, and ulcers have been confirmed to be more effective than traditional homeostatic treatments (Elliott, 2001).

Such time-dependent biochemical processes and pathophysiological phenomena exist ubiquitously, from local cells to the whole body. In summary, the occurrence of biorhythms is physiologically indispensable in life processes, and provides several advantages (Moser et al., 2006):

- Stability maintenance in response to endogenous and exogenous variations by fine-tuning the characteristics at various levels, such as cellular, organic, and holistic systems, for controlling long-term physiological functionality;
- Synchronization and coordination of different visceral organs, enabling the system to function most efficiently;
- Temporal compartmentalization, mediating polar events, such as systole and diastole, inspiration and expiration, work and rest, waking and sleeping, which cannot happen simultaneously, to occur both in alternation and efficiently in the same physical space.

The discovery of biorhythmic patterns and their perturbation is essential not only for proper diagnosis and treatment of patients suffering from various diseases, but also for daily health management of healthy persons. The following section describes our studies and the results of the long-term monitoring of various biorhythms.

2. Our Studies

The natural world is teeming with cyclic patterns and sequential events, and biorhythms are known to be important in treating disease and managing health. However, monitoring vital signs continuously in a daily life environment over a long period is a tedious task indeed. People can put up with such unpleasant assignments without much complaint over a short time period if they are on a course of treatment. However, in cases where they have no obvious symptoms, and are asked to do so purely for health care purposes, such boring daily duties will soon cause people to run out of patience.
The purposes of our studies were twofold:

- To develop convenient ways to monitor vital signs that were suitable for utilization in daily life environments for any time period without much discomfort to the user.
- To assess biorhythms through various mathematical approaches from the large amount of physiological data collected daily over a long period.

Two modes of study model are presented below. The first part describes the detection of multiple biorhythms from a single vital sign, while the second part reports on the detection of a single biorhythm from multiple vital signs.

2.1 Discovery of multiple biorhythms from a single vital sign

Multiple biorhythms are usually interwoven within an identical vital sign. This section describes the detection of different biorhythms, i.e., sleep patterns, behavioural changes, and menstrual cycles using different mathematical approaches from heart rate data collected during sleep.

2.1.1 Data collection

Heart rate data were collected during sleep using the scheme shown in Figure 3. The subject slept wearing a wrist-type Bluetooth-enabled SpO2 sensor (Model 4100, Nonin Corp., USA). A bedside box situated nearby the bed was always on stand-by waiting for the SpO2 sensor to initiate. When the SpO2 sensor was switched on, the Bluetooth wireless connection between the bedside box and the SpO2 sensor device was established automatically. With the help of the bedside box, HR and SpO2 data were collected from the SpO2 sensor via the Bluetooth connection and were transmitted continuously to a database server by an HTTP connection through an ADSL LAN in the home during a given sleep episode. When the subject rose and removed the sensor in the morning, the Bluetooth connection was closed, the bedside box went into stand-by mode, and the data collection procedure was terminated. Although the sensor collected both HR and SpO2 data simultaneously, only the HR data were used in this study. A single night's sample of collected raw HR data is shown in the black trace in Figure 4. The frequent interruption of noise spikes was perhaps due to movement artefacts, or a misinterpretation of the transmitted data package. Such noise has to be suppressed before biorhythm detection is conducted.

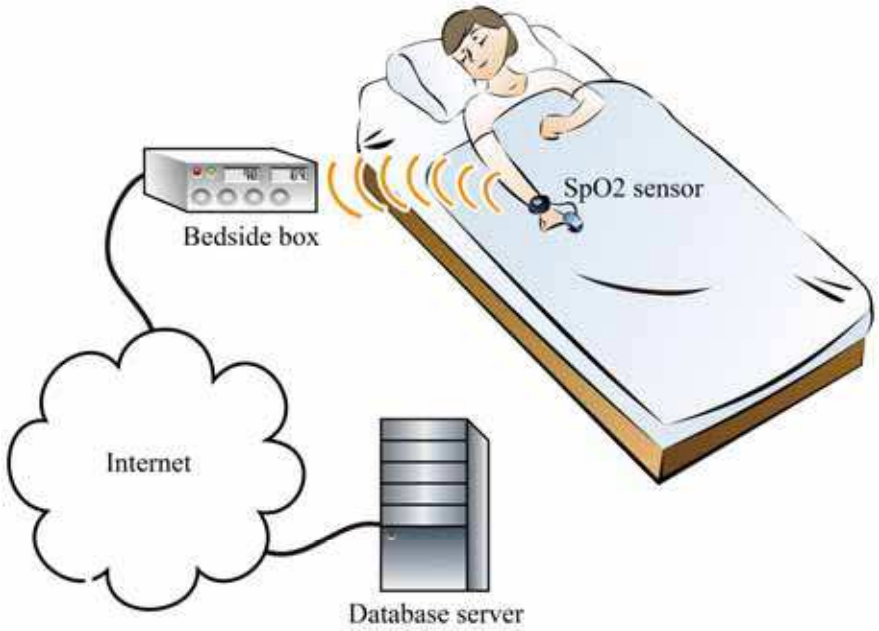

Fig. 3. Schematic drawing showing HR and SpO2 data collection during sleep. By attaching a Bluetooth-enabled SpO2 sensor to a fingertip, the nearby bedside box established a Bluetooth connection with the sensor automatically, and received HR and SpO2 data from the sensor simultaneously. These data were transmitted continuously to a database server via an HTTP connection.

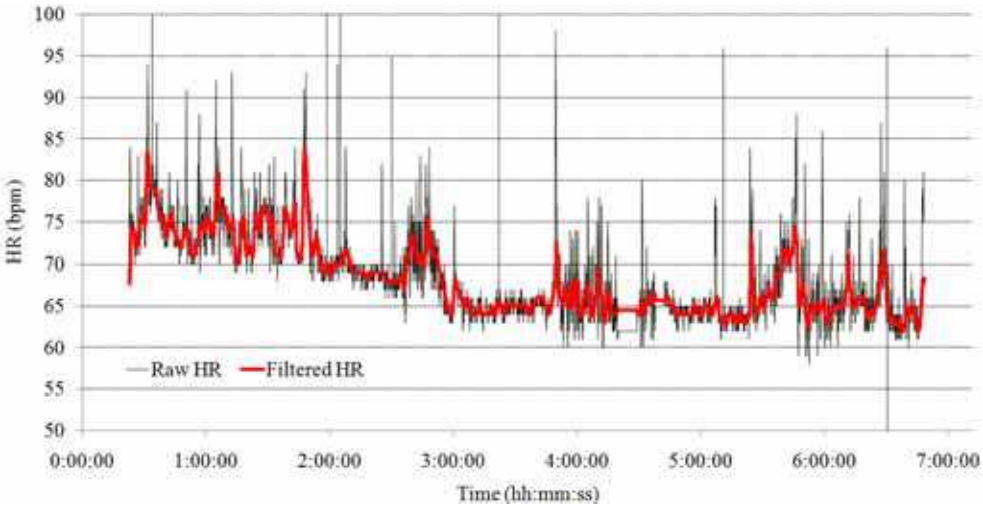

Fig. 4. Raw HR data (thin black trace) and filtered HR data (bold red trace) over a single night's sleep. Raw data were collected by a SpO2 sensor from a fingertip. Filtered data were obtained by applying a median filter and a Savitzky–Golay smoothing filter.

2.1.2 Noise suppression

Unless arrhythmia occurs, the premise of smoothing is that the HR varies slowly in nature, but its measurement is often contaminated by random noise or other artefacts. As shown in the black trace in Figure 4, the main source of noise in the raw measurement during sleep is a spike-like noise.

Noise suppression was implemented using two digital filters in two steps. A median filter was used in the first step to remove the spike-like noise, and a Savitzky–Golay filter was used in the second step to smooth the HR profile.

The median filter was a non-linear digital filtering technique, usually used in the image-processing field to remove speckle noise and salt/pepper noise from images. The idea was to represent the signal by replacing an extremely large or small value with a reasonable candidate value. This is realized using a window consisting of an odd number of data. The values within the window were sorted in numerical order, and the median value, the sample in the centre of the window, was selected as the output of the filter.

When the window was moved along the signal, the output of the median filter $y(i)$ at a moment i was calculated as the median value of the input values $x(i)$ corresponding to the moments adjacent to i ranging from $-L/2$ to $L/2$.

$$y(i) = median\left(x(i - L/2), x(i - L/2 + 1), ..., x(i), ..., x(i + L/2 - 1), x(i + L/2)\right), \quad (1)$$

where L is the length of the window.

The Savitzky–Golay filter was used to smooth the signal that was outputted from the median filter. The Savitzky–Golay filter segmented the signal as frames using a moving window, and approximated the signal frames one by one using a high-order polynomial, typically quadratic or quartic (Savitzky & Golay, 1964).

Each digital filter output $z(i)$ can be expressed by a linear combination of the nearby input points as

$$z(i) = \sum_{k=-n_L}^{n_R} c_k y(i+k), \quad (1)$$

where n_L is the number of points on the left-hand side of the data point i, and n_R is the number of points on the right-hand side of i.

The Savitzky–Golay filtering process is to find a proper polynomial to fit all n_L+n_R+1 points within each window frame on the least-squares meaning, and to produce a filter output $z(i)$ as the value of that polynomial at position i.

To derive filter coefficients, c_k, we considered fitting a polynomial of degree M in i, namely $a_0+a_1i+a_2i^2+\cdots+a_Mi^M$ to the values $y_{-nL},...,y_{nR}$. Then, $z(0)$ will be the value of that polynomial at $i = 0$, namely a_0. The design matrix for this problem is

$$A_{ij} = i^j, \qquad i = -n_L, ..., 0, ..., n_R, \qquad j = 0, ..., M, \quad (1)$$

and the normal equations for the polynomial coefficients vector, $\mathbf{a}=[a_0, a_1, a_2, \cdots, a_M]'$, in terms of the input data vector, $\mathbf{y}=[y_{-nL},...,y_{nR}]'$, can be written in matrix notation as below:

$$\mathbf{A} \cdot \mathbf{a} = \mathbf{y}, \quad (1)$$

The polynomial coefficients vector, $\mathbf{a}$, becomes

$$\mathbf{a} = \left(\mathbf{A}^T \cdot \mathbf{A}\right)^{-1} \cdot \left(\mathbf{A}^T \cdot \mathbf{y}\right), \quad (1)$$

We also have the specific forms

$$\left\{\mathbf{A}^T \cdot \mathbf{A}\right\}_{ij} = \sum_{k=-n_L}^{n_R} A_{ki} A_{kj} = \sum_{k=-n_L}^{n_R} k^{i+j} \ , \tag{1}$$

and

$$\left\{\mathbf{A}^T \cdot \mathbf{y}\right\}_{j} = \sum_{k=-n_L}^{n_R} A_{kj} y_k = \sum_{k=-n_L}^{n_R} k^{j} y_k \ , \tag{1}$$

Since the filter coefficient, c_k, is the component a_0 when $\mathbf{y}$ is replaced by the unit vector $\mathbf{e}_k$, we have

$$c_k = \left\{\left(\mathbf{A}^T \cdot \mathbf{A}\right)^{-1} \cdot \left(\mathbf{A}^T \cdot \mathbf{e}_k\right)\right\}_0 = \sum_{m=0}^{M} \left\{\left(\mathbf{A}^T \cdot \mathbf{A}\right)^{-1}\right\}_{0m} k^m \ , \ -n_L \le k < n_R \ , \tag{1}$$

When the filter coefficient vector $\mathbf{c}=[c_{-nL},\ldots,c_{nR}]$ was obtained using Equation (8), the signal shown in the black trace in Figure 4 could be smoothed using Equation (2), and the result is the red trace shown in Figure 4.

After these two filtering steps, the noise-suppressed HR data were used for the detection of three different biorhythms, as described in the following three sections.

2.1.3 Sleep cycle estimation

Sleep is clinically classified into two distinct states: the rapid eye movement (REM) state and the non-rapid eye movement (NREM) state. The NREM state is further divided into four stages, 1–4, indicating four depths of sleep from shallow to deep. When drifting into sleep, a normal sleep cycle moves in a sequential progress from Stage 1 through to Stage 4 and then Stage 3 and 2 of NREM, and finally to the REM state. Each sleep cycle lasts for 90 to 120 minutes.

During the REM sleep period, rapid eye movements occur, fluctuations in breathing movements and heart-beat become severe, blood pressure rises, and involuntary muscle jerks (loss of muscular tone) occur. However, the brain is highly active, and an EEG usually records high frequencies and low amplitudes, similar to those recorded during the awake state. Vividly recalled dreams mostly occur during REM sleep. There are three to five REM episodes per night. They occur at the end of each sleep cycle, and are not always constant in length, ranging from five minutes to over an hour.

NREM sleep is physiologically different from REM sleep, and is dreamless. As the NREM sleep advances from Stages 1 to 4, the EEG signal shows a slower frequency and a higher amplitude. Breathing and heart-beat become slower and more regular, the blood pressure and body temperature decrease, and the subject is relatively still.

About 75%–80% of sleep is NREM sleep, and almost half of the total sleep time is in Stage 2 NREM. REM sleep episodes account for 20%–25% of the total sleep period. The relative amount of REM sleep varies considerably with age. As age increases, the total sleep time becomes shorter, leading to shorter NREM sleep, but no significant change in REM sleep. By contrast, infants spend about half of their sleep time in REM sleep.

Rhythmic alternation of REM and NREM states during sleep is reflected in different physiological activities, such as eye movement, muscular tone, electroencephalogram,

respiration, heart rate, blood pressure, and body temperature. These features are clinically discernible in a polysomnogram measured by attaching more than 10 sensors to a subject.

This section describes a method for estimating the cyclic property of sleep based on HR only. Because variation in HR in the REM state is much larger than that in the NREM state, variance of the HR was used as a criterion to distinguish between REM and NREM sleep states.

The windowed local variance (WLV) method is used extensively in image processing for edge detection and pattern segmentation (Bocher & McCloy, 2006a, 2006b; Law & Chung, 2007). It is defined as the variance computed for pixel values within a window of size $w \times w$ from aggregated pixel data.

This study deals with one-dimensional HR data sequences, and defines the WLV_i at data point i as shown in Equation (9).

$$WLV_i = \frac{1}{w}\sqrt{\sum_{j=i}^{i+w}\left(x_j\right)^2 - \frac{1}{w}\left(\sum_{j=i}^{i+w} x_j\right)^2}\ , \tag{1}$$

where w is the window length and x_j is the input data within the window.

Figure 5 shows the noise-suppressed HR data in the red trace and the estimated result of a biphasic sleep cycle in the blue trace. The low-level phase indicates the period with lower HR perturbation, and the high-level phase corresponds to a period with increased HR fluctuation. Although it is not yet a conclusion that there is a relationship between the REM–NREM cycle and the estimated biphasic cycle, because no concomitant EEG was recorded, it is inferred that the low-level phase may imply the NREM state, while the high-level phase refers to the REM state.

As shown in Figure 5, the period length of the high-level phase gradually increased during the course of sleep, i.e., it was short at the beginning of the sleep period and longer towards the end of the sleep period, a behaviour similar to the REM state, although confirmation of this is required from an EEG.

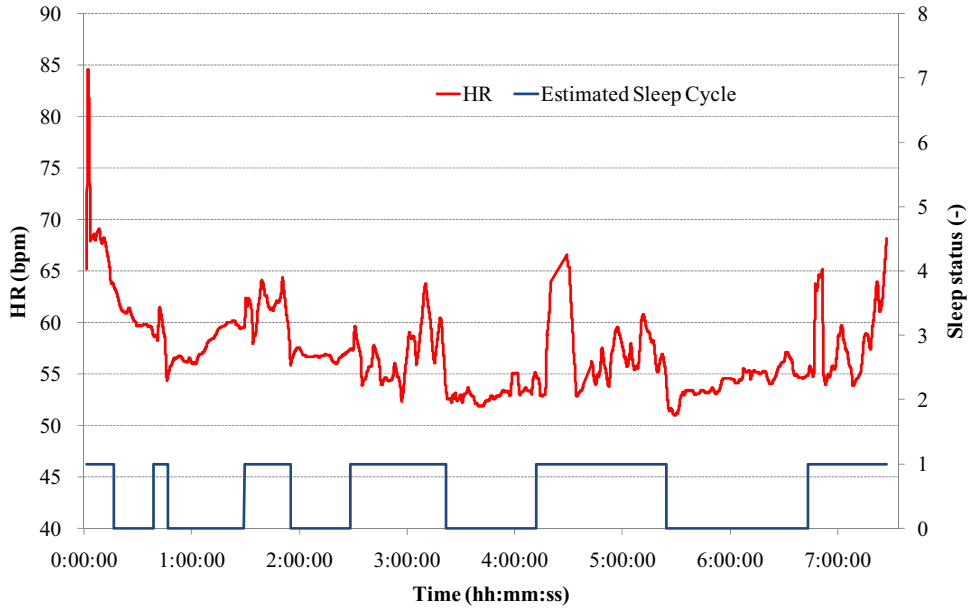

Fig. 5. HR profile of a single night's sleep and the estimated sleep cycle. Data were collected from a male student in his twenties. The red line is the profile of the noise-suppressed HR. The blue line is the estimated sleep cycle, in which the low-level phase indicates the period with low HR perturbation, and the high-level phase corresponds to the period with more HR fluctuations.

2.1.4 Detection of changes in daily behaviour

Because biorhythms are affected by endogenous and exogenous factors, any change in daily behavioural patterns can be reflected in biorhythmic changes. This study demonstrates the detection of behavioural changes during waking hours by applying the dynamic time warping (DTW) method to the HR data collected during sleep (Watanabe & Chen, 2009).

DTW is an algorithm used to measure the similarity between two data sequences that may differ in length. Well-known applications are in fields such as speech recognition and walking analysis, in which data sequences in either case generally vary in temporal span and rhythmic tempo.

The aim of DTW is to find the optimal alignment between two given data sequences under given criteria. Consider two given data sequences with variable length, the reference pattern R=$\{r_1,...,r_M\}$ with data length M, and the test pattern T=$\{t_1,...,t_N\}$ with data length N, as shown in Figure 6. The value of each black dot d_{ij} indicates the difference (distance) between the reference pattern data r_i and test pattern data t_j, as described by Equation (10).

$$d_{ij} = \sqrt{(i-j)^2 + (r_i - t_i)^2} \text{ , } i=1, 2,\ldots, M; j=1, 2,\ldots, N \text{ ,} \tag{10}$$

Thus, a two-dimensional $N \times M$ distance matrix, $D_{N\times M}$, is constructed where the element d_{ij} is the distance between the ith data in the reference pattern and the jth data in the test pattern.

As a similarity measure, the shortest path from the start (the lower left-hand corner of the distance matrix) to the end (the upper right-hand corner of the distance matrix) of the data sequence must exist among multiple possible paths.
The shortest path is determined using the forward dynamic programming approach with a monotonicity constraint.

$$P_{ij} = \min_{k \geq j} \{ d_{jk} + P_{i+1,k} \} , \quad (1)$$

Here, P_{ij} denotes the distance from the ith and jth data node to the terminating node.
The overall minimum distance, $D(T, R)$, used as the similarity measure for two patterns (a smaller distance value indicates a higher similarity) is determined from

$$D(T,R) = P_{11} , \quad (1)$$

The Sleep Index (SI) is obtained by normalizing $D(T, R)$ between the values of 0 and 1, as below:

$$SI = (D(T,R) - D_{\min}) / (D_{\max} - D_{\min}) , \quad (1)$$

where $D_{\min}$ and $D_{\max}$ indicate the minimum and maximum similarity values, respectively.
The smaller the SI value, the more regular the sleep is.

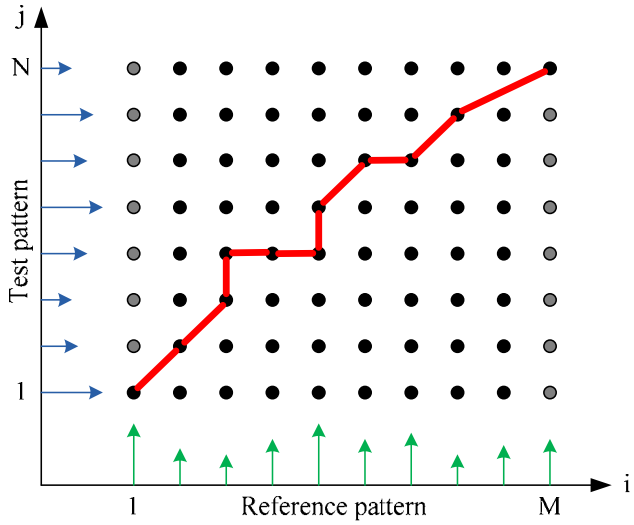

Fig. 6. The minimum distance trace (red line) from the beginning to the end of two data sequences. The black dot indicates the distance between the ith data in the reference pattern and the jth data in the test pattern. The value of the minimum distance, $D(T, R)$, is the sum of all the black dots along the red line, and indicates the similarity between the two patterns. The smaller the value of $D(T, R)$, then the greater the similarity is between the two patterns. All the data in the two data sequences were calculated to build a two-dimensional $N \times M$ distance matrix. Because the endpoint had constraints, the grey-coloured dots can be ignored.

The reference pattern was created by selecting one week's usual sleep data, and averaging these daily HR profiles after noise suppression and data length unification. The daily SI value was calculated using the daily HR profile and the reference pattern. The smaller the SI value, the greater the similarity was between the daily pattern and the reference pattern. Figure 7 shows the variation in the SI value over a period of seven weeks. SI values less than 0.6 indicate that daily sleep was relatively stable, but three days had SI values above 0.6. These three days were confirmed as coinciding with daily life behavioural changes, or heavy drinking in year-end and New Year parties. The HR data showed an increase as a whole and a marked variation pattern over these three days, suggesting that perhaps the use of alcohol stimulated the sympathetic nervous system and accelerated the heart-beat.

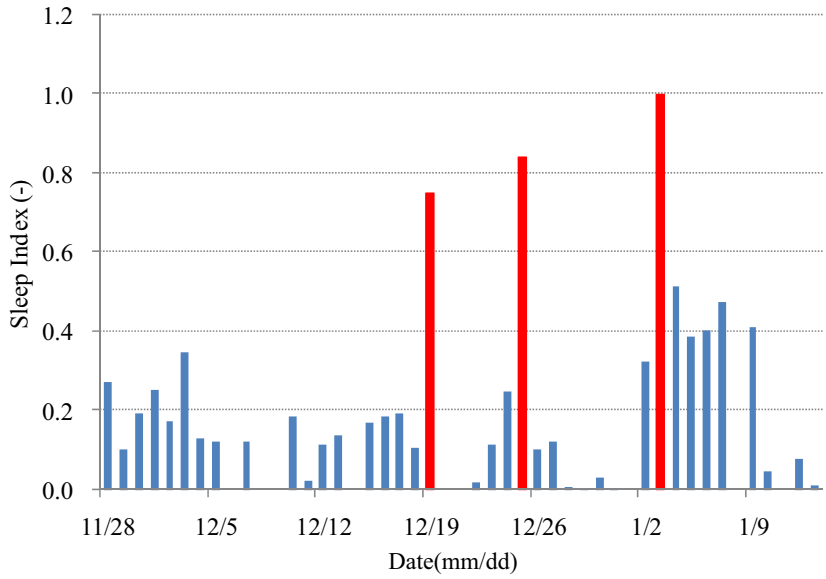

Fig. 7. Variation in SI over a period of seven weeks. The SI value was calculated using the DTW method from HR data collected from a male student in his twenties. The lower the value of the bar, the higher the similarity was, which in turn implies usual daily behaviour. The three higher red bars, whose values are greater than 0.6, indicate the days when the subject had a heavy intake of alcohol.

2.1.5 Estimation of the menstrual cycle

The menstrual cycle is usually estimated from the oral basal body temperature (BBT) in clinical practice. However, taking daily oral measurements is inconvenient for most women. By contrast, there are many convenient ways to measure HR. This study investigated whether the variation in HR measured during sleep could reveal menstrual rhythmicity, as oral BBT does.

The menstrual cycle was estimated by following three steps: calculation of the HR statistic profile, preprocessing of the profile, and analysis of the profile rhythmicity.

The first step was to calculate the daily HR mode value (most frequent value) from the noise-suppressed HR data over a single night, i.e., more than 20,000 HR data points during a 6–7-hour sleep episode. The second step had two tasks: (i) to smooth the daily HR mode profile using a Savitzky–Golay filter, and (ii) to remove any ultra-slow baseline deviations (which may imply seasonal biorhythmic changes and remain to be studied further in detail) using a multirate filtering approach. The final step was to estimate the rhythmicity from the detrended profile of the daily HR mode value using the cosinor analysis method.

The cosinor analysis method is often used to estimate biorhythms with regular cycle length from biological time series data (Nelson et al., 1979). Our aim was to look for the optimal parameter set (M, A, ω, φ) to represent the measured data using a cosine function, as shown in Equation (14)

$$f(t_i) = M + A\cos(\omega t_i + \varphi)\,, \tag{1}$$

where t_i represents the time of measurement of the ith data, M is the mean level (Midline Estimating Statistic Of Rhythm (MESOR)) of the cosine curve, A is the amplitude of the function, ω is the angular frequency (reciprocal of the cycle length) of the curve, and φ is the acrophase (horizontal shift) of the curve.

Considering the measurement of y_i to be the sum of $f(t_i)$ at time t_i and the residual error ε_i

$$y_i = M + A\cos(\omega t_i + \varphi) + \varepsilon_i\,, \tag{1}$$

The errors ε_i were assumed to be independent and normally distributed with a zero mean value and a common residual variance, σ^2.

The task was to find the optimal parameter set (M, A, ω, φ) that best fitted the measurement data y_i using Equation (15), and could be realized using the least-squares regression method. Equation (15) was rewritten as below.

$$y_i = M + A\cos\varphi\cos\omega t_i - A\sin\varphi\sin\omega t_i + \varepsilon_i\,, \tag{1}$$

Assigning surrogate parameters (β, γ), we obtain

$$\beta = A\cos\varphi \text{ and } \gamma = -A\sin\varphi\,, \tag{1}$$

$$x_i = \cos\omega t_i \text{ and } z_i = \sin\omega t_i\,, \tag{1}$$

Substituting Equations (17) and (18) into Equation (16), we get

$$y_i = M + \beta x_i + \gamma z_i + \varepsilon_i\,, \tag{1}$$

Supposing ω in Equation (18) has been suggested previously, and y_i in Equation (19) becomes a linear equation of M, β, and γ. Once M, β, and γ are calculated by applying the least-squares method to Equation (19), the optimal parameter set (M, β, γ) can be obtained.

The residual sum of squared (RSS) error is

$$RSS = \sum_{i=1}^{n}\left[y_i - (M + \beta x_i + \gamma z_i)\right]^2\,, \tag{1}$$

where n is the data length.

To minimize the value of RSS, Equation (20) is partially differentiated with respect to M, β, and γ. The following normal simultaneous equations can be established.

$$\begin{cases} nM + \left(\sum_{i=1}^{n} x_i\right)\beta + \left(\sum_{i=1}^{n} z_i\right)\gamma = \sum_{i=1}^{n} y_i \\ \left(\sum_{i=1}^{n} x_i\right)M + \left(\sum_{i=1}^{n} x_i^2\right)\beta + \left(\sum_{i=1}^{n} x_i z_i\right)\gamma = \sum_{i=1}^{n} x_i y_i \\ \left(\sum_{i=1}^{n} z_i\right)M + \left(\sum_{i=1}^{n} x_i z_i\right)\beta + \left(\sum_{i=1}^{n} z_i^2\right)\gamma = \sum_{i=1}^{n} z_i y_i \end{cases}, \quad (1)$$

After the parameter set (M, β, γ) is derived from the simultaneous equations (21), the value of *RSS* can be calculated using Equation (20). The values of A and φ can be calculated using Equation (17) as below:

$$A = \sqrt{\beta^2 + \gamma^2}\,, \quad (1)$$

$$\varphi = \arctan\left(\frac{\gamma}{\beta}\right), \quad (1)$$

Because the value of *RSS* depends on the proposed value of ω, the optimal value of ω, which has the minimum value of *RSS*, is chosen as the estimated cycle length.

Figure 8 shows the HR mode value and standard deviation profiles over a period of six months (upper subplot), and the menstrual cycle estimation procedure (lower subplot).

The HR data were collected from a female subject in her thirties during daily sleep from 8 October to 31 March. The data collection rate was 93.2% (i.e., 164 days collected out of a total 176-day period). The starting dates of the subject's menstruation were recorded by the subject as 15 October, 12 November, 9 December, 7 January, 5 February, 3 March, and 30 March. Each menstrual cycle over the six-month period could be deduced as being 28, 27, 29, 29, 26, and 27 days, respectively, and the average length ± the standard deviation of the self-recorded menstrual cycles was 27.7 ± 1.2 days.

The daily HR mode value and standard deviation were calculated from more than 20,000 HR data points during the 6–7-hour measurements of a single night's sleep episode. As shown in the upper subplot of Figure 8, the fluctuation of the raw HR mode value profile (MVP) shows no apparent regularity along the time axis.

The lower subplot shows the smoothed HR MVP data (bold blue line) obtained by applying the Savitzky–Golay smoothing filter to the raw HR MVP data. A slow wandering baseline in the smoothed HR MVP data was extracted using the multirate filter and subtracted from the smoothed HR MVP data to produce the detrended HR MVP data (dotted black line). The cosinor analysis method was used to calculate the best approximation (bold red line) of the detrended HR MVP data and to obtain the best-fitted menstrual cycle length of 24.9 days. This compares with the average self-recorded menstrual cycle length of 27.7 days, i.e., the mathematically estimated menstrual length induced an estimation error of 10.1%. It was observed that the timing of the self-recorded menstruation starting dates corresponded to the decrease phase in HR MVP data approximately, a similar characteristic which is shown in BBT biphasic data.

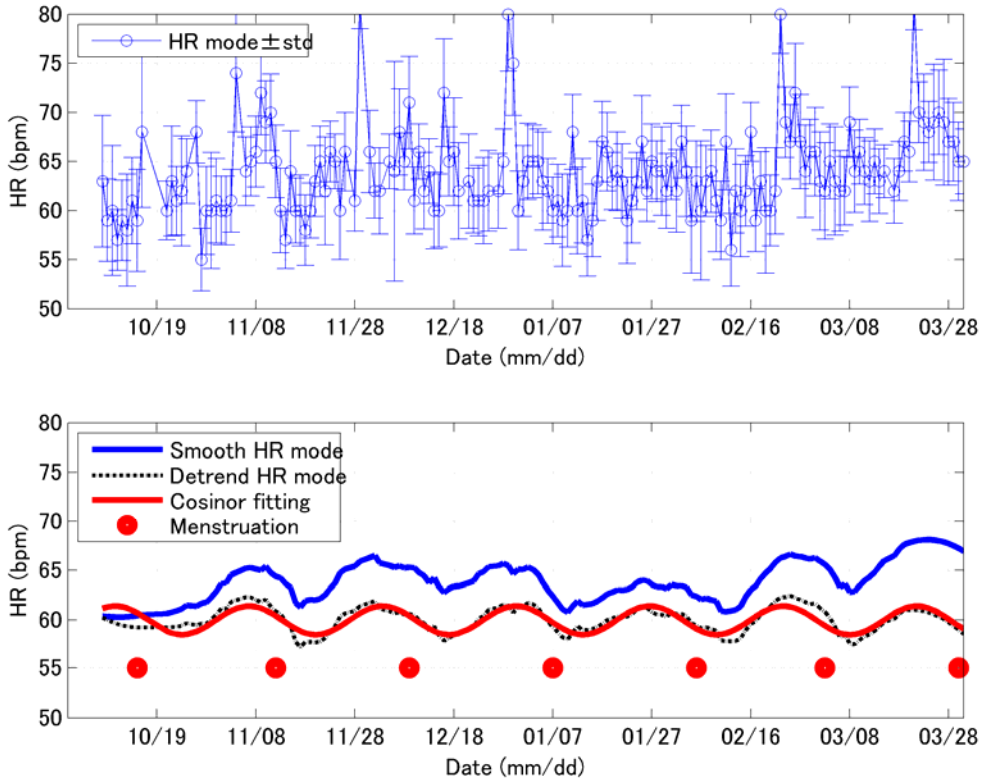

Fig. 8. HR mode value and standard deviation profiles (upper subplot), and menstrual cycle estimation procedure (lower subplot). Data are plotted based on the day-by-day data along the x-axis. The y-axis denotes HR in units of bpm. In the upper subplot, the data markers "o" and vertical bars "|", terminated at the upper and lower ends by short horizontal lines "-", show the mode values (most frequent values) and standard deviation of the HR data in daily sleep episodes. Some sporadic discontinuities can be seen, as no data were collected during those days. In the lower subplot, the bold blue line shows the smoothed profile of the daily HR mode values, and the black dotted line shows the detrended result of the smoothed HR mode values. The red line is the cosinor-fitted results of the black dotted line. Red circles denote the menstruation starting dates that were self-recorded by the subject.

The cosinor analysis method does not require that the data be sampled at equal intervals, and it also tolerates incidents of missing data. It provides an accessible means of estimating the periodic property of menstrual cycles. However, the cosinor analysis method postulates that the data should be reasonably represented in a deterministic cyclic form with a constant period. This prerequisite makes it unsuitable for those women with irregular menstrual cycles. To deal with irregular cycle cases, a hidden Markov model (HMM)-based method is presented in the next section.

2.2 Discovery of a single biorhythm from multiple vital signs

This section describes the estimation of a biphasic property, indicating ovulation and menstruation periods, in female menstrual cycles by applying the HMM method to three types of body temperature data: the oral basal body temperature (BBT), the skin body temperature (SBT), and the core body temperature (CBT).

Menstrual cycle dynamics, from ovum production to development, maturation, release, and fertilization, are one of the most important mechanisms in maintaining female mental and physical well-being, as well as reproductive function. This cyclic phenomenon is marked by changes in several physiological and hormonal signs. Throughout the menstrual cycle, changes occur in a variety of hormones, such as the luteinizing, follicle stimulating, progestational (luteal), and oestrogen (follicular) hormones, as shown in Figure 9. These changes are known to be reflected by changes in BBT measurements or in the chemical composition of the urinary metabolites of oestrogen and progesterone, cervical mucus, and saliva (Sund-Levander et al., 2002).

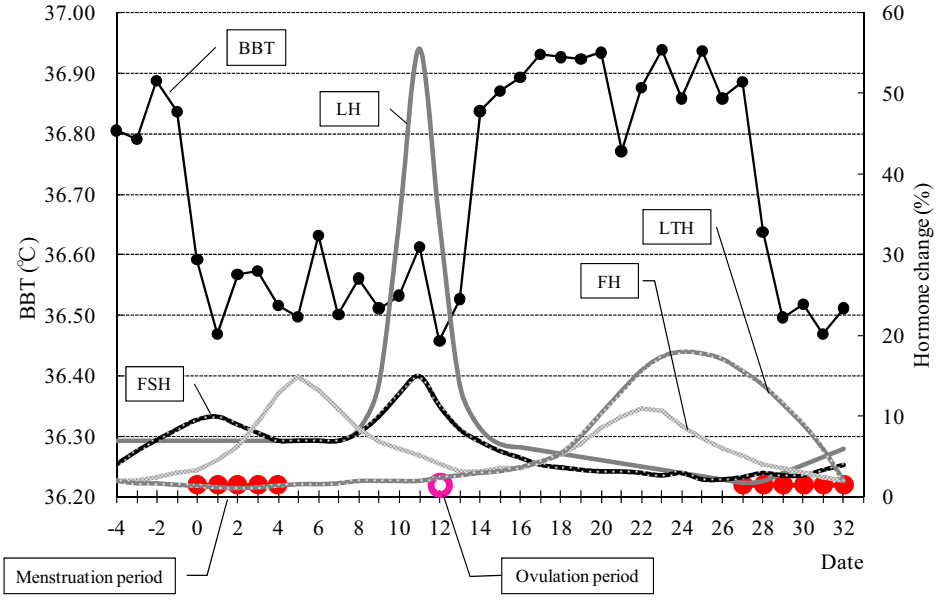

Fig. 9. Biphasic profile of the basal body temperature (BBT) and related hormone changes during a menstrual cycle. LH and LTH are the luteinizing hormone and luteal hormone, respectively, and FH and FSH are the follicular hormone and follicle-stimulating hormone, respectively. The menstruation period is indicated by the red dots, and ovulation day is marked by the pink circle. During the ovulation period, the surge in LH triggers the release of the ovum. If there is no chance of fertilization occurring within a period of one day, the ovum will shrink and form lutein cells. The concentration of LTH will increase and lead to a rise in BBT.

It is possible to correlate hormonal secretion with changes in the genital tissues during a normal menstrual cycle by employing modern bioassay techniques. Three different methods (biological, biochemical, and biophysical) have been developed to elucidate the cyclic

properties of ovulation day and the menstruation period during menstrual cycles (Collins, 1982). Urine and cervical mucus examination methods require chemical reagents and a complicated operation. The salivary method is vulnerable to influence from alcohol, smoke, and food. Cervical mucus and BBT are reported to be the most readily observable parameters among several physiological and hormonal signs (Owen, 1975; Royston, 1982).

Studies on the cause of body temperature changes in women, including BBT, CBT, and rectal temperature, can be traced back to the 1930s (Davis & Fugo, 1948; Lee, 1988; Zuck, 1938). Changes in body temperature, from lower to higher or vice versa, are indicative of the hormonal changes that lead to ovulation and menstruation. Because the BBT method only requires regular oral temperature measurements immediately following sleep, it is now widely accepted as a practical method for estimating the menstrual cycle. However, as BBT measurements are easily affected by any phlogistic illness, such as influenza or toothache, the biphasic property is often ambiguous, and it is difficult to decide the transition points from the temperature profile by visual observation. Therefore, the result largely depends on individual knowledge and a subjective judgement. Extreme caution is required in the interpretation of BBT data when evaluating menstrual cycle dynamics (Baker & Driver, 2007; Moghissi, 1980).

The aims of this study were twofold. The first was to examine whether an HMM-based method was applicable for estimating the biphasic property of menstrual cycles. The second was to investigate whether the same biorhythmic story can be told by different forms of body temperature data, which are measured at different times, at different sites, and using different techniques.

2.2.1 Data collection

Three forms of body temperature data were collected from each subject. As shown in Figure 10, both the SBT and the CBT were collected automatically by attaching two sensor devices (QOL Co. Ltd, 2009) on two sides of a drawers strap during sleep.

The SBT device (orange ellipse in Figure 10) was programmed to measure the skin body temperature at 10-minute intervals from midnight to 6:00 a.m. Measurement outliers above 40 °C or below 32 °C due to poor contact or movement artefacts were automatically disregarded. In the end, 37 data points at most can be collected during a six-hour period. The collected temperature data were encoded as a two-dimensional bar code, known as a "Quick Response" (QR) code (Denso Wave Inc., 2009) and displayed on an LCD window. A mobile phone built-in camera was used to capture the QR code image (Figure 10 (a)) on the device display (middle cycle). Once the QR code was captured on the mobile phone (Figure 10 (b)), the original temperature data (Figure 10 (c)) were recovered from the captured image and transmitted to a database server via HTTP protocol through a mobile network for data storage and analysis.

The CBT device (black cube in Figure 10) was developed using the zero-heat-flow principle (Kobayashi et al., 1975; Togawa, 1985; Nemoto & Togawa, 1988; Yamakage & Namiki, 2003). The device measured the deep tissue temperature at four-minute intervals following the first reading, which was obtained 90 minutes after the device was switched on. This was to ensure that the heat flow was balanced. The CBT data were collected using the electro-magnetic coupling method employing a docking station connected to a PC via an RS232 interface.

Oral BBT was measured by inserting a digital thermometer ("C520", Terumo Corp.) into the hypoglottis each morning immediately the subject wakes up.
Menstruation periods were recorded by the subject. Ovulation days were examined around the middle of the menstrual cycle using a diagnostic test kit ("Dotest LH", Rohto Pharmaceutical Co., Ltd), which identified the changes in concentration of LH, whose secretion increases suddenly before ovulation in a woman's urine. The day when a positive result was detected in the test was considered as the ovulation day.

Fig. 10. A schematic drawing of the CBT and SBT data collection. Both the CBT and the SBT were measured automatically by clipping two wearable devices on a drawers strap on two sides of the subject's waist during sleep. The black cubic device was used for CBT data collection. The orange elliptic device was used to detect the SBT.

Figure 11 shows sample profiles of SBT and CBT data collected from a female subject in her thirties. The variation in the amplitude of the SBT even during sleep reached 1.5 °C, while the variation in the amplitude of the CBT was about half this value. This phenomenon is also shown in Figure 13. The different behaviour of the SBT and CBT is perhaps due to the SBT measurements being much more sensitive to the degree of contact with the skin, and this leads to many more artefacts.

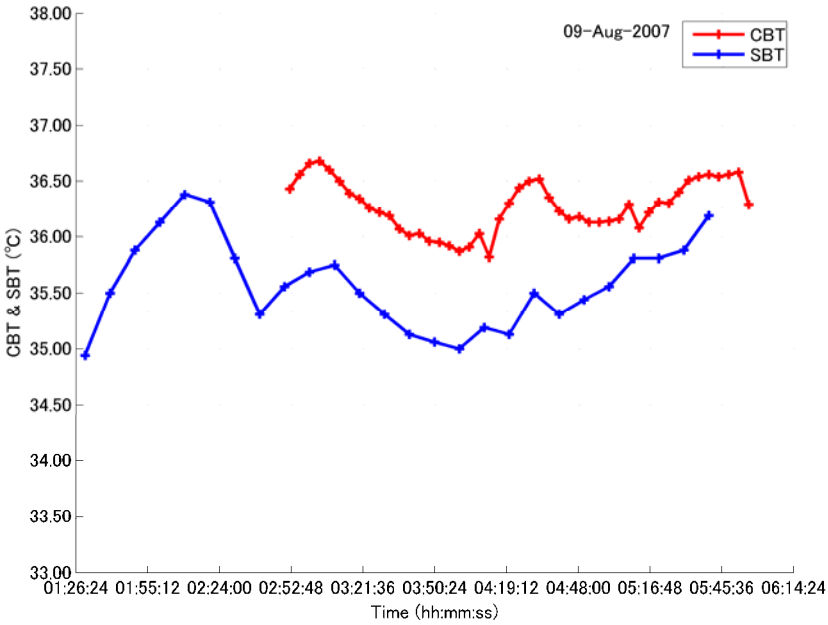

Fig. 11. A night's profile of the SBT (blue line) and CBT (red line) measured during sleep. The SBT data were collected every 10 minutes, and the CBT data were collected every four minutes after obtaining the first reading 90 minutes after the device was turned on.

2.2.2 Data analysis

The biphasic property of body temperature in a menstrual cycle was modelled using a discrete hidden Markov model (HMM) with two hidden phases: a lower temperature (LT) phase and a higher temperature (HT) phase, as shown in Figure 12.

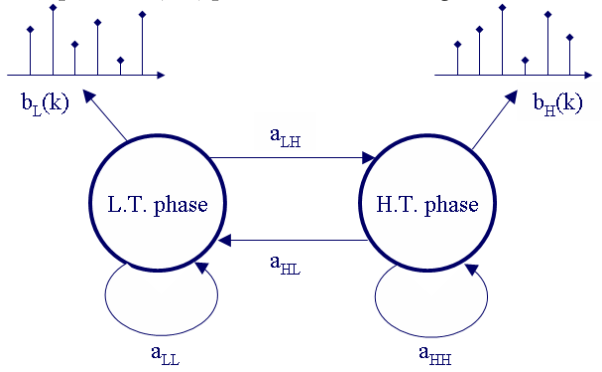

Fig. 12. A discrete HMM with two hidden phases for modelling the biphasic property of body temperature in a menstrual cycle. The term a_{LH} and similar terms represent the phase transition probability from the LT phase to the HT phase, and vice versa. The term $b_L(k)$ denotes the probability of a measurement data point *k* coming from the LT phase. The term $b_H(k)$ denotes the probability of a measurement data point *k* coming from the HT phase.

The biphasic property of the body temperature profile was estimated by finding the optimal HMM parameter set $\lambda(A,B,\pi)$ that determined the hidden phase from which each datum arose. The parameter set of an HMM is assigned randomly in the initial condition, and is optimized through the forward–backward iterative procedure until $P(O \mid \lambda)$, the probability of the measured temperature data originating from the HMM model with an assumed parameter set $\lambda(A,B,\pi)$, converges to a stable maximum value, or until the absolute logarithm of the previous and current difference in $P(O \mid \lambda)$ is not greater than the value of δ.
The algorithms for calculating the forward variable, α, the backward variable, β, and the forward–backward variable, γ, are shown in Equations (24) to (26).
The forward variable, $\alpha_t(i)$, denotes the probability of phase q_i at time t based on a partial observed temperature data sequence, $O_1,O_2,\ldots,O_t$, until time t, and can be calculated using the following steps for a given set of $\lambda(A,B,\pi)$.

$$\alpha_t(i) = P_r(O_1, O_2, ..., O_t, i_t = q_i \mid \lambda)$$

$$\alpha_1(i) = \pi_i b_i(O_1), \quad 1 \le i \le N, t = 1$$

$$\alpha_{t+1}(j) = \left[\sum_{i=1}^{N} \alpha_t(i) a_{ij}\right] b_j(O_{t+1}), \quad 1 \le j \le N, t = 1,2,...,T-1 \qquad (24)$$

The backward variable, $\beta_t(i)$, denotes the probability of phase q_i at time t based on a partial observed temperature data sequence, $O_{t+1},O_{t+2},\ldots,O_T$, from time t+1 to T, and can be calculated using the following steps for a given set of $\lambda(A,B,\pi)$.

$$\beta_t(i) = P_r(O_{t+1}, O_{t+2}, ..., O_T \mid i_t = q_i, \lambda)$$

$$\beta_T(i) = 1, \quad 1 \le i \le N, t = T$$

$$\beta_t(i) = \sum_{j=1}^{N} a_{ij} b_j(O_{t+1}) \beta_{t+1}(j), \quad 1 \le i \le N, t = T-1, T-2, ..., 1 \qquad (25)$$

To find the optimal sequence of hidden phases for a measured temperature sequence, O, and a given model, $\lambda(A,B,\pi)$, there are multiple possible optimality criteria.
Choosing the phases q_t that are individually most likely at each time t, i.e., maximizing $P(q_t = i \mid O,\lambda)$, is equivalent to finding the single best phase sequence (path), i.e., maximizing $P(Q \mid O,\lambda)$ or $P(Q,O \mid \lambda)$. The forward–backward algorithm is then applied to find the optimal sequence of phases q_t at each time t, i.e., maximize $\gamma_t(i) = P(q_t = i \mid O,\lambda)$ for a measured temperature sequence, O, and a given parameter set, $\lambda(A,B,\pi)$.

$$\gamma_t(i) = P(q_t = i \mid O, \lambda),$$

$$= \frac{P(O, q_t = i \mid \lambda)}{P(O \mid \lambda)} = \frac{P(O, q_t = i \mid \lambda)}{\sum_{i=1}^{N} P(O, q_t = i \mid \lambda)}$$
$$= \frac{P(o_1 o_2 ... o_t, q_t = i \mid \lambda) P(o_{t+1} o_{t+2} ... o_T \mid q_t = i, \lambda)}{\sum_{i=1}^{N} P(o_1 o_2 ... o_t, q_t = i \mid \lambda) P(o_{t+1} o_{t+2} ... o_T \mid q_t = i, \lambda)}$$
$$= \frac{\alpha_t(i)\beta_t(i)}{\sum_{i=1}^{N} \alpha_t(i)\beta_t(i)} \quad , \tag{26}$$

The most likely phase q_t^* at time t can be found as

$$q_t^* = \arg\max_{1 \le i \le N} [\gamma_t(i)], \quad 1 \le t \le T \quad , \tag{27}$$

There are no existing analytical methods to optimize $\lambda(A,B,\pi)$, so that $P(O \mid \lambda)$ or $P(O,I \mid \lambda)$ is usually maximized (i.e., $\lambda^* = \arg\max_{\lambda} [P(O \mid \lambda)]$ or $\lambda^* = \arg\max_{\lambda} [P(O, Q \mid \lambda)]$,) using gradient techniques and an expectation-maximization method. In this study, the Baum–Welch method was used because of its numerical stability and linear convergence (Rabiner, 1989).

To update $\lambda(A,B,\pi)$ using the Baum–Welch re-estimation algorithm, we defined the variable $\xi_t(i,j)$ to express the probability of a datum being in phase i at time t and phase j at time t+1, given the model parameter set and the temperature data sequence, as

$$\xi_t(i,j) = P(q_t = i, q_{t+1} = j \mid O, \lambda) = \frac{P(q_t = i, q_{t+1} = j, O \mid \lambda)}{P(O \mid \lambda)} \quad , \tag{28}$$

From the definitions of the forward and backward variables, $\xi_t(i,j)$ and $\gamma_t(i)$ are related as

$$\xi_t(i,j) = \frac{\alpha_t(i) a_{ij} b_j(o_{t+1}) \beta_{t+1}(j)}{P(O \mid \lambda)} = \frac{\alpha_t(i) a_{ij} b_j(o_{t+1}) \beta_{t+1}(j)}{\sum_{i=1}^{N} \sum_{j=1}^{N} \alpha_t(i) a_{ij} b_j(o_{t+1}) \beta_{t+1}(j)} \quad , \tag{29}$$

$$\gamma_t(i) = P(q_t = i \mid O, \lambda) = \sum_{j=1}^{N} P(q_t = i, q_{t+1} = j \mid O, \lambda) = \sum_{j=1}^{N} \xi_t(i,j) \quad , \tag{30}$$

where $\sum_{t=1}^{T-1} \gamma_t(i)$ indicates the expected number of transitions from phase i in O, and $\sum_{t=1}^{T-1} \xi_t(i,j)$ indicates the expected number of transitions from phase i to phase j in O.

Therefore, $\lambda(A,B,\pi)$ can be updated using Equations (31)–(33) as follows.

As π_i is the initial probability and indicates the expected frequency (number of times) in phase i at time t = 1, $\pi_i = \gamma_1(i)$, it can be used to calculate the forward and backward variables.

$$\pi_i = \frac{\alpha_1(i)\beta_1(i)}{\sum_{i=1}^{N}\alpha_1(i)\beta_1(i)} = \frac{\alpha_1(i)\beta_1(i)}{\sum_{i=1}^{N}\alpha_T(i)}, \tag{31}$$

where a_{ij} is the transition probability from phase i to phase j and can be calculated from the expected number of transitions from phase i to phase j divided by the expected number of transitions from phase i.

$$a_{ij} = \frac{\sum_{t=1}^{T-1}\xi_t(i,j)}{\sum_{t=1}^{T-1}\gamma_t(i)} = \frac{\sum_{t=1}^{T-1}\alpha_t(i)a_{ij}b_j(o_{t+1})\beta_{t+1}(j)}{\sum_{t=1}^{T-1}\alpha_t(i)\beta_t(i)}, \tag{32}$$

where $b_j(k)$ is the expected number of data arising from phase j, divided by the expected number of all measured data arising from phase j, and can be calculated by

$$b_j(k) = \frac{\sum_{\substack{t=1 \\ s.t.O_t=o_k}}^{T}\gamma_t(j)}{\sum_{t=1}^{T}\gamma_t(j)}, \tag{33}$$

The initial input quantities are the known data N (number of hidden states), M (number of discrete temperature data), T (number of temperature data), O (symbolized temperature data), and the randomly initialized $\lambda(A,B,\pi)$. Once the values of α, β, and γ are calculated using Equations (24) to (26), then $\lambda(A,B,\pi)$ is updated using Equations (31) to (33) employing the newly obtained values of α, β, and γ. The search for the optimal parameter set, λ_{opt}, is terminated when $P(O|\lambda)$ converges to a stable maximum value, or when the absolute logarithm of the previous and current $P(O|\lambda)$ difference reaches δ. Thus, the most likely phase from which a datum is observed can be estimated using Equation (27).

2.2.3 Results

The HMM approach was applied to three types of body temperature data series, BBT, CBT, and SBT, which were measured using different techniques on different sites and at different times, respectively. Figure 13 shows the same story of female body rhythmicity (menstrual cycle) along with different body temperature measurements, and examines the algorithmic performance of the biphasic property estimation by comparing the menstruation records and ovulation test results.

Clinically, the transition point from the HT to the LT phase during a biphasic menstrual cycle corresponds to the menstruation period, and ovulation should occur with a coincidence of the transition point from the LT to the HT phase in time.

As shown in Figure 13, among the six menstruation periods and five days of ovulation over six months, the biphasic property estimated from the BBT data coincided with all the menstruation periods and four out of five ovulation days. The single mismatch error was one day later in the estimation result than the actual ovulation day. The biphasic property derived from CBT identified all six menstruation periods and all five ovulation days, but with errors in three out of five ovulations. Because a severe artefact occurred in the SBT

measurements (perhaps due to poor contact with skin), the daily variation in the SBT data was much higher than that in both the CBT and the BBT data. Six menstruation periods were identified, but three out of five ovulations were missed in the SBT measurements. Overall, the best estimation result was obtained from the BBT measurements. The CBT data were the second best in performance, and the SBT data showed the poorest result.

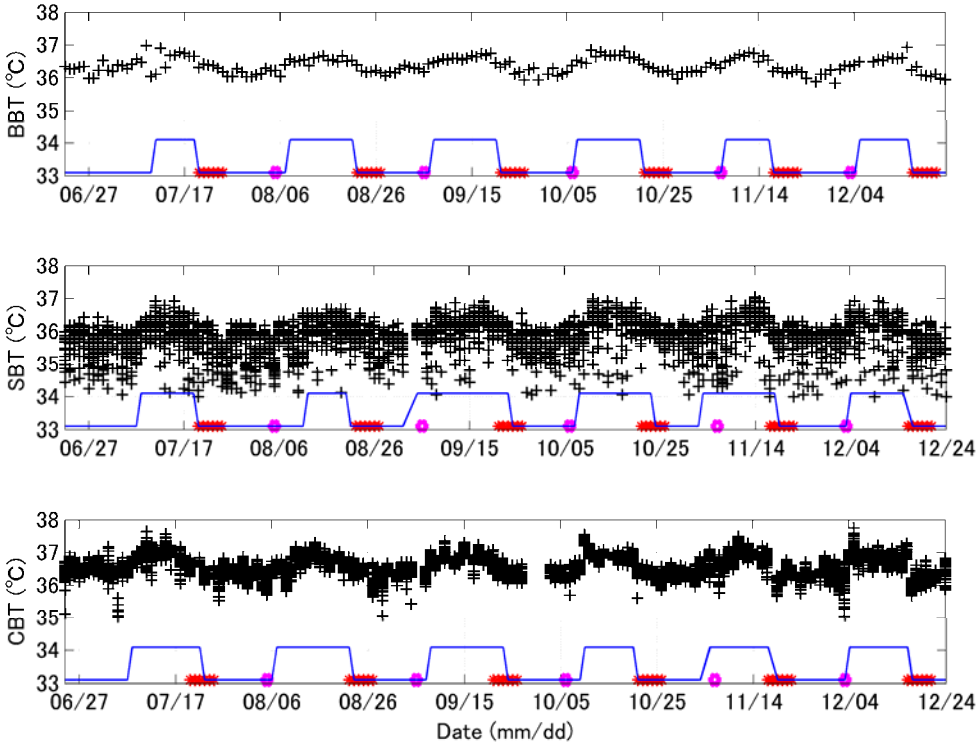

Fig. 13. Measurement of three types of body temperature data (SBT, BBT, and CBT), and the detected biphasic menstrual cycles over a period of six months. The BBT, SBT, and CBT data are plotted from top to bottom, respectively, and the data are indicated by the black markers "+". Each adjacent blue line indicates the detected biphasic menstrual cycles. The menstruation periods denoted by the red star "*" were recorded by subject. Ovulation days are denoted by the pink circle, and were determined by using a commercially available kit "Dotest LH" utilizing the LH secretion test. Physiologically, the transient point from the HT to the LT phase corresponds to a menstruation period, and the transient point from the LT to the HT phase corresponds to the ovulation day.

3. Discussion

Cosmic and hominine rhythms exist eternally and ubiquitously in the temporal and spatial domains. The rhythmic nature in the universe influences every aspect of animals and plants, commencing before conception and extending beyond death (Palmer, 2002; Foster &

Kreitzman, 2005). A large volume of academic understanding has been documented in the scientific literature (Refinetti, 2005).

Biorhythms are built-in genetically, and have evolved naturally through an interaction with the host's environmental factors. The range of biorhythm periods extends from milliseconds to more than a year. Individual clock cells exist genetically in many peripheral tissues, and oscillate semi-autonomously under the coordination of the SCN in the anterior hypothalamus (Shirakawa et al., 2001). Thus, a time-dependent alternation of homeostasis for different endocrine, physiological, and behavioural functions is controlled by the SCN (master clock) and the derived time instruction to the peripheral tissues (slave clocks) throughout the body (Dunlap, 1999). Biorhythmic functions within the human body demonstrate different peak–trough performances in different time slots in the course of a day, month, and year.

However, in most current clinical routines, when a sample of blood, urine, saliva, or tissue is taken, or when other vital signs, such as ECG, blood pressure, and body temperature are measured, they are evaluated as being normal or abnormal by simply comparing them with a range of values obtained statistically from a large population without any consideration of when the sample or measurement was taken, because it is supposed that human body functions are based on a homeostatic principle and are time-independent (Touitou & Haus, 1992). This doctrine has been criticized in that evaluating a patient's blood pressure using a single reading taken during an office visit is like trying to understand the plot of a film by looking at a single frame (Halberg, 1969).

Circadian rhythmic expression of most symptoms is known to worsen at night. For example, acute pulmonary oedema occurs more frequently at night (Manfredini et al., 2000). Allergic conditions such as asthma, allergic rhinitis, hay fever, and measles are exacerbated at night, during sleep, and in the early morning close to waking up compared with during the day. Similarly, symptoms of rheumatoid arthritis worsen at night and improve during the day (Bellamy et al., 2002; Cutolo et al., 2003). However, a reverse pattern can be found in migraine attacks, which occur more often in the morning immediately after waking and decrease at night (Solomon, 1992).

Circannual rhythms have also been identified in commonly used biomarkers in blood, urine, and saliva (Halberg et al., 1983). For example, sperm concentration is lowest in the summer and highest in the autumn and winter (Levine, 1999). Seasonal variations in immune defence systems, including all types of leukocytes, have been investigated (Touitou & Haus, 1994). Skin tends to be more hydrated in the summer and dryer in the winter, which is linked to an increase in the incidence of dermatitis (Mehling & Fluhr, 2006). The treatment recommended for "summer hypertension" and "winter hypertension", respectively may be opposite (Halberg et al., 2006b). In addition, human hair has been reported to reach a maximum growth rate in September and a minimum rate in January (Reinberg & Ghata, 1964).

Illnesses disrupt normal biorhythms and influence biorhythmic property parameters. Similarly, a perturbation in biorhythmic property parameters reflects a deviation from health status or the incidence of illnesses.

Since the kidney is a major organ of metabolism and detoxification, underlying circadian effects on daily biochemical and physiological processes play a key role in metabolism and detoxification. For example, one of the most important functions of antidiuretic hormone (ADH) is to regulate the body's retention of water. Its release causes the kidneys to conserve water, thus concentrating the urine and reducing urine volume. More ADH is normally

secreted at night than during the day in human beings, causing decreased urine production during the usual sleep episode. However, in older persons or patients with spinal cord injuries, there is a distorted diurnal rhythmic pattern in ADH secretion. Decreased nocturnal secretion of ADH causes increased urine production at night (nocturia) and interrupted sleep. Therefore, occurrence of an abnormal sleeping–waking pattern, i.e., frequent sleep disruption during the night may imply nocturia and kidney disorder (Szollar et al., 1997).

Recognizing biorhythms and their changes is important in interpreting and treating disease. To investigate a wide range of variations in biorhythms and their application in medicine and health care systematically, an innovative framework based upon sound definitions in the biomedical engineering domain is indispensable. It requires not only novel systematic theory and methodology for assessing complicated interactions of the time-dependent factors responsible for disease rhythmicity, but also inventive tools suitable for daily use by both medical professionals and a large population of untrained users.

It is essential that reliable information with fine temporal resolution is collected over a period long enough to allow objective characterization of an individual's periodic phenomena. Development of bioinstrumentation and sensory technologies to detect vital signs, and biochemical markers that do not present any inconvenience and are suitable for use in daily scenarios is of paramount importance.

Measurement of ECG or HR is now possible in various daily life situations. Whenever a person sits on a chair (Lim et al., 2006) or on a toilet (Togawa et al., 1989), sleeps on a bed (Kawarada et al., 2000; Chen et al., 2005), sits in a bathtub (Mizukami et al., 1989; Tamura et al., 1997), or even takes a shower (Fujii et al., 2002), then the ECG and HR data can be monitored without any inconvenience or discomfort.

The smart dress "wealthy outfit" weaves electronics and fabrics together to detect the wearer's vital signs, and transmits the data wirelessly to a computer. The built-in sensors gather information on the wearer's activities, ECG, and body temperature. Despite having nine electrodes and conductive leads woven into it, the suit looks completely normal and is worn without any discomfort (Marculescu et al., 2003; Rossi, 2008).

The wellness mobile phone, "SH706iw", has all the standard features of a mobile phone but also acts as a pedometer, a body fat meter, and a pulse rate and breath gas monitor. Moreover, daily data can be collected using a built-in game-like application (Sharp Corp., 2008; DoCoMo Corp., 2008).

Such innovations in sensory instrumentation technologies and physiological data collection schemes are indispensable for monitoring a wide range of biorhythms in everyday living environments that are oriented to mostly untrained users. Other key features should include zero administration, easy manipulation, automatic fault recovery, and the absence of unpleasantness or disturbance to everyday living to allow perpetual sustainable data collection. Related studies can be classified into three groups: invisible technology that requires no user intervention during operation, wearable technology that can be worn as if a part of the subject's underwear with little discomfort, and ubiquitous technology that is based on mobile devices for instant usage, at any time and in any place (Chen et al., 2008).

Moreover, automatic and continuous monitoring during sleep at night is worth paying special attention to, because not only is the sleeping–waking cycle important in keeping biorhythms in tune, but also much reliable physiological data can be obtained due to fewer movement artefacts. In addition, the attenuation in some biorhythms during sleep helps the

decoupling of overlapping multiple biorhythms and potential masking factors that usually only appear during diurnal measurements.

Further, not only the temporal alternations in the daily and seasonal domain, but also cycles of meteorological and geographical events, such as the solar wind, sun spots, and geomagnetic storms, have an important effect on human body functions (Halberg et al., 2006b). While keeping watch over diverse biorhythms, nature's clocks do not oscillate in isolation. Substantial improvements in daily data aggregation should include collective information, such as meteorological, environmental, and geographical aspects at the same time as the physiological data. This will facilitate the disentangling of diverse causal pathways of many endogenous and exogenous factors within biorhythms, as well as the interrelationships among different biorhythms and natural rhythms across the wide range of temporal and spatial factors.

The discovery of more biorhythms largely depends on learning how to take full advantage of the broad spectrum of accumulated data from a large population over a long period, and how to perform multiple modalities of data fusion through the integration of sound mathematical models and the implementation of robust computational algorithms.

As human beings evolve through an interaction with nature, human physiological functions become more organized and more complicated. Underlying biorhythmic processes in disease manifestation are complex and multifaceted. Although human beings have now become accustomed to the 24-hour light–dark cycle, circadian and other biorhythmic patterns are interwoven with each other and have been incorporated into a single vital sign or biochemical marker. These insights suggest that the separate computational models that have been developed for a single biorhythm will have to be integrated for solving multiple biorhythms. The emerging field of intelligent data mining and algorithm development for identification of hidden biorhythms and the separation of interlaced multiple biorhythms will complement established work in chrono-related medical science.

Chronopharmacology helps to explain the biorhythm dependencies of medications. Comprehensive investigation into biorhythms can assist us to synchronize the rhythmic variation in individual physiological functions while being related to pharmacokinetics, which will tell us how the body responds to a drug, and to pharmacodynamics, which will tell us how the drug affects the body (Redfern & Lemmer, 1997).

Treatment in the evening is associated with an elevation in the circadian amplitude of BP, which in turn may induce iatrogenic CHAT in some patients, thereby unknowingly increasing the risk of cardiovascular disease (Halberg et al., 2006b). It is not wise to lower the risk of hypertension, and instead introduce a higher risk of CHAT, which is like attending to one condition while worsening another.

Abnormalities in the variability of blood pressure and similar signs are difficult to find in a sporadic clinical examination, and the efficacy of treatment is difficult to optimize by relying on a spot check, which is driven by convenience rather than pertinence. Instead, through chronobiology, by interpreting their circadian or preferably longer rhythms, it is possible to comprehend the change of related illnesses in different temporal scales, over a day or over years, and to increase the impact on effectiveness of a treatment through scheduling the time of medication.

The optimal strategy for chronotherapy and administration of treatment for diseases requires clarification of each medication in terms of the best timing and dosage, such as when the drug is interacting with the body most efficiently, with the maximum positive

effect and the minimum adverse effect, and when the most appropriate amounts of the drug should be delivered to the desired target organ along a temporal course.
Timed-delay medication technology and automatic drug delivery devices play an important role in the optimal individualization of a treatment (Lemmer, 2007). Major approaches for drug delivery include oral, pulmonary, and transdermal routes. Microcapsules ingested by mouth can travel freely throughout the body, seek the target organ automatically, and deliver therapeutic agents at a desired time (Orive et al., 2004). Microneedles and electric field-driven polymers can diffuse therapeutic agents to target tissues from scheduled temporal profiles through the skin barrier as a means of penetrating plaques on vessel walls (Reed et al., 1998).
Prominent application of biorhythms in health care, disease prevention, and diagnosis, as well as the timing of treatments and drug regimens will gradually mature and be extensively recognized through diligent efforts and intense collaborations among multiple disciplines.

4. Conclusions

Historical endeavours in the study of biorhythms from both the oriental and the occidental worlds, especially the achievements over the last 60 years, and their application in medicine and health care, have been briefly reviewed in this chapter. A wide range of inherent biorhythm diversity exists and is subject to the influence of various endogenous and exogenous aspects. The destruction or asynchronism of biorhythms will harm human health. Likewise, any indisposition in health will be reflected in biorhythmic fluctuations. To identify various biorhythms and to facilitate their application in medical practice and daily life, convenient monitoring and comprehensive interpretation of long-term physiological data are indispensable. Our exploration has focused on the development of advanced sensory technology and data mining algorithms. These devices are suitable for the continuous monitoring of vital signs over long periods in a daily life environment. The algorithms developed for discovering a wide range of biorhythms were confirmed using long-term physiological data.
Through an investigation of the interplay among biorhythm behaviours, health status, and the intrinsic timing of disease development, a treatment strategy, such as dosage and dosing regimen to maximize the therapeutic effects, guarantee medication safety, and minimize adverse effects, can be optimized using automatic drug delivery technologies. In addition, health care performance and efficiency can be achieved by adapting human activity to the synchronization of organ physiological functions and environmental aspects.

5. Acknowledgements

The author thanks colleagues and students from universities and companies for co-work in the above studies, and thanks participants for their enduring efforts in long-term data collection. These studies were supported in part by several financial resources from: (a) The Innovation Technology Development Research Program under JST (Japan Science and Technology Agency) grant H17-0318; (b) MEXT Grants-In-Aid for Scientific Research No. 20500601; and (c) The University of Aizu Competitive Research Funding P-24.

6. References

Baker, F. C. & Driver, H. S. (2007). Circadian rhythms, sleep, and the menstrual cycle. *Sleep Medicine*, Vol. 8, No. 6, pp. 613-622.

Balsalobre, A.; Brown, S.A.; Marcacci, L.; Tronche, F.; Kellendonk, C.; Reichardt, H.M.; Schütz, G. & Schibler, U. (2000). Resetting of Circadian Time in Peripheral Tissues by Glucocorticoid Signaling. *Science*, Vol. 289. No. 5488, pp. 2344-2347

Bellamy, N.; Sothern, R.B.; Campbell, J. & Buchanan, W.W. (2002). Rhythmic variations in pain, stiffness, and manual dexterity in hand osteoarthritis. *Annals of the Rheumatic Diseases*, Vol. 61, pp. 1075-1080

Biochart Com. (2009). Biorhythms History. http://www.biochart.co.uk/biorhythms-history.shtml

Bocher, P. K. & McCloy, K. R. (2006a). The fundamentals of average local variance - part I: detecting regular patterns. *IEEE Transactions on Image Processing*, Vol. 15, No. 2, pp. 300-310.

Bocher, P.K. & McCloy, K. R. (2006b). The fundamentals of average local Variance-part II: sampling simple regular patterns with optical imagery. *IEEE Transactions on Image Processing*, Vol. 15, No. 2, pp. 311-318.

Chen, W.; Zhu, X.; Nemoto, T.; Kanemitsu, Y.; Kitamura, K. & Yamakoshi, K. (2005). Unconstrained detection of respiration rhythm and pulse rate with one under-pillow sensor during sleep. *Medical & Biological Engineering & Computing*, Vol. 43, No. 2, pp. 306–312.

Chen, W.; Zhu, X.; Nemoto, T.; Wei, D. & Togawa, T. (2008). A Scalable Healthcare Integrated Platform (SHIP) and Key Technologies for Daily Application, *Data Mining in Medical and Biological Research*, IN-TECH, 978-953-7619-30-5, Vienna, Austria, pp. 177-208.

Chirkova, É. N. (1995). Mathematical methods of detection of biological and heliogeophysical rhythms in the light of developments in modern heliobiology: A platform for discussion. *Cybernetics and Systems Analysis*, Vol. 31, No. 6, pp. 903-918.

Chou, B. J. & Besch, E. L. (1974). A computer method for biorhythm evaluation and analysis. *Biological Rhythm Research*, Vol. 5, No. 2, pp. 149-160.

Collins, W. P. (1982). Ovulation prediction and detection. *IPPF Med. Bull.*, Vol. 16, pp. 1–2.

Cutolo, M.; Seriolo, B.; Craviotto, C.; Pizzorni, C. & Sulli, A. (2003). Circadian rhythms in RA. *Annals of the Rheumatic Diseases*, Vol. 62, pp. 593-596.

Davis, M. E. & Fugo, N. W. (1948). The cause of physiologic basal temperature changes in women. *J. Clin. Endocrinol.*, Vol. 8, pp. 550–563.

Denso Wave Inc. (2009). QR code, http://www.denso-wave.com/qrcode/aboutqr-e.html.

Desai, V. G.; Moland, C. L.; Branham, W. S.; Delongchamp, R. R.; Fang, H.; Duffy, P. H.; Peterson, C. A.; Beggs, M. L. & Fuscoe, J. C. (2004). Changes in expression level of genes as a function of time of day in the liver of rats. *Mutation Res.*, Vol. 549, No. 1-2, pp. 115-129.

DoCoMo Corp., (2008). Wellness mobile phone. http://www.nttdocomo.co.jp/product/foma/706i/sh706iw/index.html

Dunlap, J.C. (1999). Molecular Bases for Circadian Clocks – Review. *Cell*, Vol. 96, pp. 271–290.

Dunlap, J.C.; Loros, J.J. & Decoursey, P.J. (2004). *Chronobiology: Biological Timekeeping*, Sinauer Associates, 087893149X, Massachusetts, USA.

Elliott, W. J. (2001). Timing treatment to the rhythm of disease: A short course in chronotherapeutics. *Postgraduate medicine*, Vol. 110, No. 2, pp. 119-122, 125-126, 129

Foster, R.G. & Kreitzman, L. (2005). *Rhythms of Life: The Biological Clocks that Control the Daily Lives of Every Living Thing*, 0-300-10969-5, Yale University, New Haven, USA.

Fujii, M.; Dema, H. & Ueda, T. (2002). Liquid Jet Electrode and Surface Potential Detector, *Japanese Patent* No. JP2002–65625A, 5 March 2002.

Halberg, F.; Halberg, E.; Barnum, C.P. & Bittner, J.J. (1959). Physiologic 24-hour periodicity in human beings and mice, the lighting regimen and daily routine. In: Withrow RB (ed). *Phototperiodism and Related Phenomena in Plants and Animals*. Ed. Publ. No. 55. Washington, D.C., pp. 803-878.

Halberg, F. (1969). Chronobiology. *Ann. Rev. Physiol*., Vol. 31, pp. 675-725.

Halberg, F. (1983). Quo vadis basic and clinical chronobiology: promise for health maintenance. *Am. J. Anat*., Vol. 168, pp. 543-594.

Halberg, F.; Lagoguey, M. & Reinberg, A. (1983). Human circannual rhythms over a broad spectrum of physiological processes. *International journal of chronobiology*, Vol. 8, No. 4, pp. 225-268

Halberg, F. & Cornélissen, G. (1993). Rhythms and blood pressure. *Ann. 1st. Super. Sanita*, Vol. 29, No. 4, pp.647–665.

Halberg, F.; Cornélissen, G.; Katinas, G.; Syutkina, E.V.; Sothern, R.B.; Zaslavskaya, R.; Halberg, F.; Watanabe, Y.; Schwartzkopff, O.; Otsuka, K.; Tarquini, R.; Frederico, P. & Siggelova, J. (2003). Transdisciplinary unifying implications of circadian findings in the 1950s. *Journal of Circadian Rhythms*, Vol. 1, No. 2, pp. 1-61.

Halberg, F.; Cornélissen, G.; Katinas, G.; Tvildiani, L.; Gigolashvili, M.; Janashia, K.; Toba, T.; Revilla, M.; Regal, P.; Sothern, R.B.; Wendt, H.W.; Wang, Z.; Zeman, M.; Jozsa, R.; Singh, R.B.; Mitsutake, G.; Chibisov, S.M.; Lee, J.; Holley, D.; Holte, J.E.; Sonkowsky, R.P.; Schwartzkopff, O.; Delmore, P.; Otsuka, K.; Bakken, E.E.; Czaplicki, J. & the International BIOCOS Group. (2006a). Chronobiology's progress. Part I, season's appreciations 2004–2005: time-, frequency-, phase-, variable-, individual-, age- and site-specific chronomics. *J. Appl. Biomed*., Vol. 4, pp. 1–38.

Halberg, F.; Cornélissen, G.; Katinas, G.; Tvildiani, L.; Gigolashvili, M.; Janashia, K.; Toba, T.; Revilla, M.; Regal, P.; Sothern, R.B.; Wendt, H.W.; Wang, Z.; Zeman, M.; Jozsa, R.; Singh, R.B.; Mitsutake, G.; Chibisov, S.M.; Lee, J.; Holley, D.; Holte, J.E.; Sonkowsky, R.P.; Schwartzkopff, O.; Delmore, P.; Otsuka, K.; Bakken, E.E.; Czaplicki, J. & the International BIOCOS Group. (2006b). Chronobiology's progress. Part II, chronomics for an immediately applicable biomedicine. *J. Appl. Biomed*., Vol. 4, pp. 73–86.

Hufeland, C.W. (1796). Art of Prolonging Life. http://www.archive.org/details/artofprolongingl00hufeuoft

Katz, G.; Durst, R.; Zislin, Y.; Barel, Y. & Knobler, H. Y. (2001). Psychiatric aspects of jet lag: review and hypothesis. *Medical Hypotheses*, Vol. 56, pp. 20-23

Kawarada, A.; Nambu, M.; Tamura, T.; Ishijima, M.; Yamakoshi, K. & Togawa, T. (2000). Fully automated monitoring system of health status in daily life, *Proceedings of the 22nd Annual International Conference of the IEEE Engineering in Medicine and Biology Society*, Vol. 1, pp. 531–533.

Kobayashi, T.; Nemoto, T.; Kamiya, A. & Togawa, T. (1975). Improvement of Deep Body Thermometer for Man. *Annals of Biomedical Engineering*, Vol. 3, pp. 181-188.

Koukkari, W.L. & Sothern, R.B. (2006). *Introducing Biological Rhythms: A Primer on the Temporal Organization of Life, with Implications for Health, Society, Reproduction, and the Natural Environment*, Springer, 978-1-4020-3691-0, New York, USA

Kumar, K., Srivastava, M. & Mandal, S. K. (1992). A Multivariate Method for the Parameter Estimation in Biorhythms. *Biometrical Journal*, Vol. 34, No. 8, pp. 911–917.

Labrecque, G. & Belanger, P. M. (1991). Biological rhythms in the absorption, distribution, metabolism and excretion of drugs. *Pharmacol. Ther.*, Vol. 52, No. 1, pp. 95–107.

Law, M.W.K. & Chung, A.C.S. (2007). Weighted Local Variance-Based Edge Detection and Its Application to Vascular Segmentation in Magnetic Resonance Angiography. *IEEE Transactions on Medical Imaging*, Vol. 26, No. 9, pp. 1224–1241.

Lee, K. A. (1988). Circadian temperature rhythms in relation to menstrual cycle phase. *J. Biol. Rhythms.*, Vol. 3, pp. 255–263.

Lemmer, B. (1994). Chronopharmacology: time, a key in drug treatment. *Ann. Biol. Clin.*, Vol. 52, No. 1, pp. 1-7.

Lemmer, B. (2007). Chronobiology, drug-delivery, and chronotherapeutics. *Adv. Drug Deliv. Rev.*, Vol. 59, No. 9-10, pp. 825-827.

Levine, R.J. (1999). Seasonal variation of semen quality and fertility. *Scand J Work Environ Health*, Vol. 25 Suppl. 1, pp. 34-37

Lim, Y.G.; Kim, K.K. & Park, K.S. (2006). ECG measurement on a chair without conductive contact, *IEEE Trans. Biomed. Eng.*, Vol. 53, No. 5, pp. 956–959.

Manfredini, R.; Portaluppi, F.; Boari, B.; Salmi, R.; Fersini, C. & Gallerani, M. (2000). Circadian Variation in Onset of Acute Cardiogenic Pulmonary Edema is Independent of Patients' Features and Underlying Pathophysiological Causes. *Chronobiology International*, Vol. 17, No. 5, pp. 705-715.

Marculescu, D.; Marculescu, R.; Park, S. & Jayaraman, S. (2003). Ready to wear, *Spectrum, IEEE*, Vol. 40, No. 10, pp. 28–32.

Martha, U. G. & Sejnowski, T. J. (2005). Biological Clocks Coordinately Keep Life on Time. *Science*, Vol. 309, pp. 1196-1198.

Mehling, A. & Fluhr, J.W. (2006). Chronobiology: biological clocks and rhythms of the skin. *Skin Pharmacol. Physiol.*, Vol. 19, No. 4, pp. 182-189.

Mizukami, H.; Togawa, T.; Toyoshima, T. & Ishijima, M. (1989). Management of pacemaker patients by bathtub ECG, *Report of the Institute for Medical & Dental Engineering, Tokyo Medical and Dental University*, 23, pp. 113–119.

Moghissi, K. S. (1980). Prediction and detection of ovulation. *Fertil. Steril.*, Vol. 32, pp. 89–98.

Moser, M.; Fruhwirth, M.; Penter, R. & Winker, R. (2006). Why life oscillates - from a topographical towards a functional chronobiology. *Cancer Causes Control*, Vol. 17, No. 4, pp. 591-599.

Naumova, E.N. (2006). Mystery of Seasonality: Getting the Rhythm of Nature. *J. Public Health Policy*, Vol. 27, No. 1, pp. 2-12.

Nelson, W.; Tong, Y.L.; Lee, J.K. & Halberg, F. (1979). Methods for cosinor-rhythmometry. *Chronobiologia*, Vol. 6, No. 4, pp. 305-323.

Nemoto, T. & Togawa, T. (1988). Improved probe for a deep body thermometer. *Medical and Biological Engineering and Computing*, Vol. 26, No. 4, pp. 456-459.

Ni, M. (1995). *The Yellow Emperor's Classic of Medicine: A New Translation of the Neijing Suwen with Commentary*, Shambhala, 978-1570620805, Massachusetts, USA.

Ohdo, S. (2007). Chronopharmacology Focused on Biological Clock, *Drug Metabolism and Pharmacokinetics*, Vol. 22, No. 1, pp.3-14

Orive, G.; Hernández, R.M.; Gascón, A.R.; Calafiore, R.; Chang, T.M.S.; Vos, P.; Hortelano, G.; Hunkeler, D.; Lacík, I. & Pedraz, J.L. (2004). History, challenges and perspectives of cell microencapsulation. *Trends in Biotechnology*, Vol. 22, No. 2, pp. 87-92.

Owen, J. A. Jr. (1975). Physiology of the menstrual cycle. *Am. J. Clin. Nutr.*, Vol. 28, pp. 333–338.

Palmer, J.D. (2002). *The Living Clock: The Orchestrator of Biological Rhythms*, Oxford University Press, 978-0195143409, New York, USA.

QOL Co. Ltd., (2009). Ran's Night. http://rans-night.jp/

Rabiner, L. R. (1989). A tutorial on hidden Markov models and selected applications in speech recognition. *Proc. IEEE*, Vol. 77, No. 2, pp. 257–286.

Redfern, P.H. & Lemmer, B. (1997). *Chronopharmacology: Physiology and Pharmacology of Biological Rhythms*, Springer, 978-3540615255, New York, USA.

Reed, M.L.; Wu, C.; Kneller, J.; Watkins, S.; Vorp, D.A.; Nadeem, A.; Weiss, L.E.; Rebello, K.; Mescher, M.; Smith, A.J.C.; Rosenblum, W. & Feldman, M.D. (1998). Micromechanical Devices for Intravascular Drug Delivery. *Journal of Pharmaceutical Sciences*, Vol. 87, No. 11, pp. 1387-1394.

Refinetti, R. (2005). *Circadian Physiology*, CRC, 2nd edition, 978-0849322334, FL. USA.

Reinberg, A. & Ghata, J. (1964). *Biological rhythms*, Walker, New York, USA

Reppert, S.M. & Weaver, D.R. (2001). Molecular analysis of mammalian circadian rhythms. *Annu. Rev. Physiol.*, Vol. 63, pp. 647-676.

Rossi, D. D. (2008). Ready to wear: clothes that look hip and track your vital signs, too. http://www.wired.com/techbiz/startups/magazine/16-02/ps_smartclothes, *Wired Magazine*, Vol. 16, No. 2, p. 55.

Royston, J. P. (1982). Basal body temperature, ovulation and the risk of conception, with special reference to the lifetimes of sperm and egg. *Biometrics*, Vol. 38, pp. 397–406.

Sacred Lotus Arts. (2009). The Origins of Traditional Chinese Medicine. http://www.sacredlotus.com/theory/yinyang.cfm

Savitzky, A. & Golay, M. J. E. (1964). Smoothing and Differentiation of Data by Simplified Least Squares Procedures. *Analytical Chemistry*, Vol. 36, No. 8, pp. 1627–1639.

Sharp Corp., (2008). Wellness mobile phone. http://plusd.itmedia.co.jp/mobile/articles/0805/27/news064.html

Shirakawa, T.; Honma, S. & Honma, K. (2001). Multiple oscillators in the suprachiasmatic nucleus. *Chronobiology International*, Vol. 18, No. 3, pp. 371-387.

Smolensky, M. H. & Labrecque, G. (1997). Chronotherapeutics. *Pharmaceutical News*, Vol. 4, pp. 10-16.

Smolensky, M. & Lamberg, L. (2000). *The Body Clock Guide to Better Health: How to Use Your Body's Natural Clock to Fight Illness and Achieve Maximum Health*, Henry Holt and Company, 978-0-8050-5662-4, New York, USA.

Solomon, G.D. (1992). Circadian rhythms and migraine. *Cleveland Clinic Journal of Medicine*, Vol. 59, No. 3, pp. 326-329.

Stetson, M.H. & Watson-Whitmyre, M. (1976). Nucleus suprachiasmaticus: the biological clock in the hamster? *Science*, Vol. 191, No. 4223, pp. 197-199.

Sund-Levander, M.; Forsberg, C. & Wahren, L. K. (2002). Normal oral, rectal, tympanic and axillary body temperature in adult men and women: a systematic literature review. *Scand J. Caring Sci.*, Vol. 16, No. 2, pp. 122-128.

Szollar, S.M.; Dunn, K.L.; Brandt, S. & Fincher, J. (1997). Nocturnal polyuria and antidiuretic hormone levels in spinal cord injury. *Archives of Physical Medicine and Rehabilitation*, Vol. 78, No. 5, pp. 455-458.

Tamura, T.; Yoshimura, T.; Nakajima, K.; Miike, H. & Togawa, T. (1997). Unconstrained heart-rate monitoring during bathing. *Biomedical Instrumentation & Technology*, Vol. 31, No. 4, pp. 391–396.

Togawa, T. (1985). Body temperature measurement. *Clin. Phys. Physiol. Meas.*, Vol. 6, pp. 83-108.

Togawa, T.; Tamura, T.; Zhou, J.; Mizukami, H. & Ishijima, M. (1989). Physiological monitoring systems attached to the bed and sanitary equipments. *Proceedings of the Annual International Conference of the IEEE Engineering in Engineering in Medicine and Biology Society*, Vol. 5, pp. 1461–1463.

Touitou, Y. & Haus, E. (1992). *Biologic Rhythms in Clinical and Laboratory Medicine*, Springer, 978-3540544616, New York, USA.

Touitou, Y. & Haus, E. (1994). Aging of the Human Endocrine and Neuroendocrine Time Structure. *Annals of the New York Academy of Sciences*, Vol. 719, pp. 378-397.

Turek, F. W. & Allanda, R. (2002). Liver has rhythm. *Hepatology*, Vol. 35, pp. 743–745.

Vallot, J.; Sardou, G. & Faure, M. (1922). De l'influence des taches solaires: sur les accidents aigus des maladies chroniques. *Gazette des Hôpitaux*, pp. 904–905.

Veith, I. (2002). *The Yellow Emperor's Classic of Internal Medicine*, University of California Press, 979-0520229364, California, USA.

Wakuda, Y.; Noda, A.; Sekiyama, K.; Hasegawa, Y. & Fukuda, T. (2007). Biorhythm-Based Awakening Timing Modulation. *IEEE International Conference on Robotics and Automation*, pp. 1232–1237.

Wang, H.T. (2005). *Lectures on "The Medical Classic of Emperor Huang"*, People's Medical Publishing House, 711704862X/R.4863, Beijing, China

Watanabe, H. & Chen, W. (2009). Detection of Biorhythm Change from Pulse Rate Measured during Sleep. *Proc. of 48th Japan Soc. ME & BE conference*, pp. 298.

Wikipedia. (2009a). Alexander Chizhevsky. http://en.wikipedia.org/wiki/Alexander_Chizhevsky

Wikipedia. (2009b). Circadian rhythm. http://en.wikipedia.org/wiki/Circadian_rhythm

Wikipedia. (2009c). Jean-Jacques d'Ortous de Mairan. http://en.wikipedia.org/wiki/Jean-Jacques_d'Ortous_de_Mairan

Wikipedia. (2009d). Medical Classic of Emperor Huang. http://en.wikipedia.org/wiki/Huangdi_Neijing

Wikipedia. (2009e). Sanctorius. http://en.wikipedia.org/wiki/Sanctorius

Wikipedia. (2009f). Yin and yang. http://en.wikipedia.org/wiki/Yin_yang

Wikipedia. (2009g). Zhang Zhongjing. http://en.wikipedia.org/wiki/Zhang_Zhongjing

Xuan, W.; Yuan, C.S.; Bieber, E.J. & Bauer, B. (2006). *Textbook of Complementary and Alternative Medicine*, 2nd Edition, Informa HealthCare, 978-1842142974, London, UK.

Yamakage, M. & Namiki, A. (2003). Deep temperature monitoring using a zero-heat-flow method. *Journal of Anesthesia*, Vol. 17, No. 2, pp. 108-115.

Zhang, C.J.; Xu, G.Q. & Zong, Q.H. (1995). *Commentaries of Medical Classic of Emperor Huang*, People's Medical Publishing House, 7-117-00789-3/R.790, Beijing, China

Zuck, T. T. (1938). The relation of basal body temperature to fertility and sterility in women. *Am. J. Obstet. Gynecol.*, Vol. 36, pp. 998–1005.

Recent Advances in Biomedical Engineering

Edited by Ganesh R Naik

ISBN 978-953-307-004-9
Hard cover, 660 pages
Publisher InTech
Published online 01, October, 2009
Published in print edition October, 2009

The field of biomedical engineering has expanded markedly in the past ten years. This growth is supported by advances in biological science, which have created new opportunities for development of tools for diagnosis and therapy for human disease. The discipline focuses both on development of new biomaterials, analytical methodologies and on the application of concepts drawn from engineering, computing, mathematics, chemical and physical sciences to advance biomedical knowledge while improving the effectiveness and delivery of clinical medicine. Biomedical engineering now encompasses a range of fields of specialization including bioinstrumentation, bioimaging, biomechanics, biomaterials, and biomolecular engineering. Biomedical engineering covers recent advances in the growing field of biomedical technology, instrumentation, and administration. Contributions focus on theoretical and practical problems associated with the development of medical technology; the introduction of new engineering methods into public health; hospitals and patient care; the improvement of diagnosis and therapy; and biomedical information storage and retrieval. The book is directed at engineering students in their final year of undergraduate studies or in their graduate studies. Most undergraduate students majoring in biomedical engineering are faced with a decision, early in their program of study, regarding the field in which they would like to specialize. Each chosen specialty has a specific set of course requirements and is supplemented by wise selection of elective and supporting coursework. Also, many young students of biomedical engineering use independent research projects as a source of inspiration and preparation but have difficulty identifying research areas that are right for them. Therefore, a second goal of this book is to link knowledge of basic science and engineering to fields of specialization and current research. The editor would like to thank the authors, who have committed so much effort to the publication of this work.

How to reference

In order to correctly reference this scholarly work, feel free to copy and paste the following:

Wenxi Chen (2009). Discovery of Biorhythmic Stories behind Daily Vital Signs and Its Application, Recent Advances in Biomedical Engineering, Ganesh R Naik (Ed.), ISBN: 978-953-307-004-9, InTech, Available from: http://www.intechopen.com/books/recent-advances-in-biomedical-engineering/discovery-of-biorhythmic-stories-behind-daily-vital-signs-and-its-application

INTECH
open science | open minds

InTech Europe
University Campus STeP Ri
Slavka Krautzeka 83/A

InTech China
Unit 405, Office Block, Hotel Equatorial Shanghai
No.65, Yan An Road (West), Shanghai, 200040, China

51000 Rijeka, Croatia
Phone: +385 (51) 770 447
Fax: +385 (51) 686 166
www.intechopen.com

中国上海市延安西路65号上海国际贵都大饭店办公楼405单元
Phone: +86-21-62489820
Fax: +86-21-62489821